HOCHSCHULE OSNABRÜCK
UNIVERSITY OF APPLIED SCIENCES

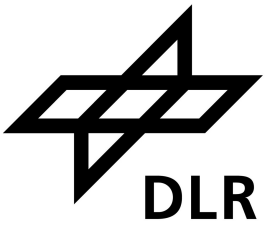

Design and Validation of an AI based Plant Stress Detection System in the EDEN ISS Environment

Faculty of Engineering and Computer Science
of the Osnabrück University of Applied Sciences
Study program "Distributed and Mobile Applications"

Master-Thesis

to reach the academic degree
Master of Science

submitted by

Leander Nordmann

Student number:	684256
Date of announcement:	01.02.2024
Date of submission:	01.07.2024
First auditor:	Prof. Dr. Clemens Westerkamp
Second auditor:	Ferdinand Rewicki

Acknowledgements

I would like to express my deepest gratitude to everyone who supported me during my Master's thesis. First, I thank my supervisor at DLR, Ferdinand Rewicki, for his calm behavior, encouragement, and constructive feedback. Your commitment was crucial to the success of this work. I would also like to extend my special thanks to my academic supervisor, Professor Clemens Westerkamp, for his valuable advice and support. A heartfelt thanks goes to the German Aerospace Center for their financial support and for providing the necessary resources for this research. I am deeply grateful to my family and friends for their support, patience, and encouragement throughout this time. Your belief in me and your constant motivation have been a source of strength and inspiration. I would also like to thank my friends who assisted me by proofreading this work. Thank you all for your invaluable contributions and support. Without you, this work would not have been possible.

Abstract

This thesis explores the detection of abiotic stress in plants using the EDEN ISS dataset. It aims to develop algorithms for image preprocessing, identify key features for stress detection, and implement suitable anomaly detection methods. The primary objective is to enhance the accuracy and reliability of stress detection in controlled environments, particularly for applications in space missions where sustainable food production is essential. The report identifies the yellow pixel count and optical flow angle as critical indicators of plant stress. These features proved effective in distinguishing between healthy and stressed plants. The Green Threshold method emerged as the most efficient segmentation approach, while the Local Outlier Factor (LOF) method demonstrated high accuracy and reliability in anomaly detection. Extensive experimental tests validated the developed algorithms and models, confirming their effectiveness. The study also highlights the need for more extensive, diverse datasets. Future research should focus on expanding the dataset, improving algorithms, and automating preprocessing steps to enhance efficiency and applicability. The developed methods offer practical solutions for real-time monitoring and management of plant health in controlled environments and are particularly relevant for long-duration space missions. This research contributes significantly to controlled environment agriculture and lays the foundation for future innovations in plant stress detection.

Abstrakt

Diese Thesis untersucht die Erkennung von abiotischem Stress bei Pflanzen unter Verwendung des EDEN ISS-Datensatzes. Ziel ist es, Algorithmen für die Bildvorverarbeitung zu entwickeln, Schlüsselmerkmale zur Stresserkennung zu identifizieren und geeignete Anomalieerkennungsmethoden zu implementieren. Das Hauptziel ist die Verbesserung der Genauigkeit und Zuverlässigkeit der Stresserkennung in kontrollierten Umgebungen, insbesondere für Anwendungen in Weltraummissionen, bei denen nachhaltige Lebensmittelproduktion unerlässlich ist. Diese Arbeit identifiziert die Gelbpixelanzahl und den optischen Flusswinkel als kritische Indikatoren für Pflanzenstress. Diese Merkmale erwiesen sich als effektiv bei der Unterscheidung zwischen gesunden und gestressten Pflanzen. Die Green Threshold-Methode erwies sich als der effizienteste Segmentierungsansatz, während die Local Outlier Factor (LOF)-Methode hohe Genauigkeit und Zuverlässigkeit bei der Anomalieerkennung zeigte. Umfangreiche experimentelle Tests bestätigten die Wirksamkeit der entwickelten Algorithmen und Modelle. Die Studie hebt auch die Notwendigkeit umfangreicherer und diverserer Datensätze hervor. Zukünftige Forschung sollte sich auf die Erweiterung des Datensatzes, die Verbesserung der Algorithmen und die Automatisierung der Vorverarbeitungsschritte

konzentrieren, um Effizienz und Anwendbarkeit zu verbessern. Die entwickelten Methoden bieten praktische Lösungen für die Echtzeitüberwachung und das Management der Pflanzengesundheit in kontrollierten Umgebungen und sind besonders relevant für Langzeit-Weltraummissionen. Diese Forschung leistet einen bedeutenden Beitrag zur Landwirtschaft in kontrollierten Umgebungen und legt den Grundstein für zukünftige Innovationen in der Stresserkennung bei Pflanzen.

Contents

List of Figures

List of Tables

List of Abbreviations

BLSS Bioregenerative Life Support System
CEA Controlled Environment Agriculture
MTF Mobile Test Facility
MCC Mission Control Center
NMIII Neumayer Station III
AWI Alfred-Wegener-Institut
SES Service Section
FEG Future Exploration Greenhouse
NDVI Normalized Difference Vegetation Index
NIR Near-Infrared
GRVI Green-Red Vegetation Index
VARI Visible Atmospherically Resistant Inde
GRVI Green-Red Vegetation Index
CNN Convolutional Neural Networks
RNN Recurrent Neural Networks
LSTM Long Short-Term Memory Networks
GAN Generative Adversarial Network
LOF Local Outlier Factor
SVM Support Vector Machine
SAM Segment Anything Model
SLIC Simple Linear Iterative Clustering
PCA Principal Component Analysis

1 Introduction

In this chapter, the goals and significance of the EDEN ISS project are explored, which aims to develop automated systems for growing plants in extreme environments such as Mars or the Moon. The central research question of this thesis is: Which features and models are best suited for detecting stress in plants using the EDEN ISS dataset? This research is crucial for future space missions, as the ability to produce food autonomously is essential for long-term space travel and colonization. By leveraging advanced image processing and machine learning techniques, the study aims to identify the most effective methods for detecting abiotic stress in plants, contributing to the development of sustainable, automated farming systems in space. This chapter sets the stage for the detailed investigation and analysis, offering an overview of the research topic, motivation, problem statement, and thesis structure.

1.1 Topic and Motivation

The Eden ISS project is a significant milestone in space research, particularly in food production in extreme environments. The research focuses on cultivating plants in a controlled environment agriculture (CEA) and monitoring the CEA from a remote control center. These studies are especially relevant for manned missions involving extended stays in space or on other planets, such as Mars or the Moon. The goal is to develop an automated bio-regenerative life support system (BLSS) capable of growing plants under extreme conditions, minimizing the need for astronaut intervention while providing a sustainable cycle.
The central research question of this thesis is: Which features and models are best suited for detecting stress in plants, based on the Eden ISS dataset? This question aims to identify the most effective features for monitoring and maintaining plants in stressed conditions.
The ability to produce food autonomously for space missions to other planets is critical. Since astronauts' time is valuable, the automation of such systems is of great importance. Identifying the best features for detecting abiotic stress is a step toward fully automated, efficient plant farming systems that can operate independently of human intervention.

The survival and well-being of astronauts on long-duration missions or in colonial settlements on other planets depend on the ability to produce food locally. Plants cannot grow naturally in these extreme environments, so a deep understanding of their growth and stress detection is essential. The successful cultivation of plants in space conditions is crucial for self-sustaining life on other planets.
Ongoing projects like EDEN ISS [Ze19], Luna ISS [Sc22], and the NEXT GEN EDEN ISS [Sc22] highlight the relevance of this topic. Future NASA missions to Mars and simulations for the Artemis program [Sm20], which marks America's return to the Moon, closely link these projects. Companies like SpaceX and various international space organizations [He22] are discussing and planning the construction of settlements on the Moon and Mars, making the topic even more pressing.
This thesis contributes significantly to research by identifying and analyzing the best features for detecting abiotic stress in plants. Such insights could form the basis for future technologies in autonomous greenhouses on earth and space. The detection and analysis of plant stress using various imaging technologies is a burgeoning field within plant sciences. Stress detection methods often rely on biotic indicators like viruses or other microorganisms. However, there is a notable lack of abiotic datasets that trace stress back to specific nutrient deficiencies or other non-living factors. Hyperspectral imaging has become a prominent tool in this domain, particularly for stress detection. While ultraviolet (UV), multispectral, and infrared (IR) imaging are commonly employed, there is a significant underutilization of RGB imaging for these purposes.
Despite its potential, researchers infrequently use RGB imaging for plant stress detection. The challenges associated with accurate phenotyping based on RGB data explain this underutilization. The difficulty lies in precisely extracting phenotypic traits from RGB images, a complex process requiring advanced algorithms and robust data analysis techniques.
Research gaps remain in the effective use of RGB images to detect plant traits and their role in stress identification. The process involves several stages, from feature extraction and trait selection to developing algorithms capable of discriminating between these traits. Conversely, in-depth research into multispectral and hyperspectral imaging has shown promising results. These advanced imaging techniques allow for more precise phenotyping to provide new insights into various plant traits. These technologies can more accurately monitor changes in leaf angle, plant aging, color variation, and the effects of stress. The positive results of such studies have the potential to lay the groundwork for innovative solutions in both agriculture and space exploration, where understanding plant health and stress responses is critical.

1.2 Problem Statement

This thesis addresses the research problem of identifying optimal features for detecting abiotic stress in plants using data from the Eden ISS project. Abiotic stresses, such as temperature fluctuations, water deficits, and other environmental extremes, significantly impact plant growth and productivity. Understanding and identifying these stressors is critical for thriving plant growth in controlled environments, especially on space missions with harsh conditions and limited resources.
This research project focuses on the detection of plant stress using the EDEN ISS Greenhouse dataset. The EDEN ISS Greenhouse, located in Antarctica, serves as a preliminary step in testing plant production for extended space missions or cultivation on other planets. The greenhouse operates almost completely independently of the external environment and is monitored by a global team of experts via satellite communications. During its operation, images of the grown plants were stored and transmitted, forming the data set for this master's thesis on plant stress detection.
The primary goal of this thesis is to accurately detect anomalies and classify healthy and diseased plants over time. This overall goal breaks down into several specific sub-goals:

- Develop algorithms to pre-process images and identify key features for plant stress detection.
- Identify an appropriate machine learning model for anomaly detection within the EDEN ISS dataset.
- Conduct and evaluate experimental tests to validate the proposed hypotheses.

The scope of this study includes the analysis of plant image data collected under controlled conditions as part of the Eden ISS project. It includes identifying and evaluating features indicative of abiotic stress and the development of methods for automated stress detection. However, the study is limited to the specific environmental conditions and plant species studied in the Eden ISS project. Results may not directly apply to other environments or species without further validation and adaptation. While the study aims to propose automated systems for stress detection, the implementation and testing of these systems in actual space missions is beyond the scope of the study.
By addressing these objectives, the research aims to significantly increase the understanding of plant stressors and improve methods for detecting and managing plant health in controlled environments. These advancements could have profound implications for the viability and success of space-based agricultural systems.

1.3 Thesis Structure

The structure of this thesis is designed to systematically explore the identification and detection of abiotic stress in plants using the EDEN ISS dataset and other relevant datasets. The chapters are organized to guide the reader through the background, methodology, experimental results, and study conclusions.

First, the introductory chapter provides an overview of the research topic, including the motivation for the study, the problem statement, and an outline of the thesis structure. This sets the stage for the detailed investigation and analysis that follows. The second chapter reviews the state of the art in plant stress detection and analysis. It covers key studies and findings, highlighting gaps in current research that this thesis aims to address.

The third chapter offers the necessary background information for understanding the study. This includes an overview of the EDEN ISS project and its significance, a detailed explanation of plant stress, focusing on abiotic stress and plant stress resistance, basic concepts in image processing such as histograms, color spaces, and segmentation techniques, and an introduction to relevant machine learning methods including supervised, unsupervised, and semi-supervised learning, as well as anomaly detection techniques.

The fourth chapter describes the datasets used in the study, namely the EDEN ISS and Plant Phenotyping datasets. It includes descriptions of these datasets, their structure, and any preprocessing steps taken to ensure data quality.

The fifth chapter outlines the research methodology, detailing the overall concept and approach of the study. This includes preprocessing techniques such as tray and plant detection and segmentation, feature engineering processes including feature extraction and data analysis, and anomaly detection methods applied to identify plant stress indicators. The sixth chapter presents the experiments conducted during the study and the results obtained. This includes a comparison of different segmentation methods and detailed results from the EDEN ISS dataset, including preprocessing, feature engineering, and anomaly detection.

The seventh chapter discusses the experiments' results, interpreting the findings in the context of the research objectives. It explores the implications of the results, the limitations of the study, and potential areas for future research. Finally, the eighth chapter summarizes the main findings of the thesis, reflecting on the research questions and objectives. It provides a conclusion based on the findings and discusses potential future developments and applications of the research. This structured approach ensures an understanding of the problem, the methodology used to address it, and the lessons learned from the research, paving the way for advancements in plant stress detection in space and controlled environments.

2 Related Work

2.1 State of the Art

Recently, research in the field of plant phenotyping and stress analysis has advanced significantly, in particular through the use of cutting-edge technologies and methods. The EDEN ISS project plays a central role in testing innovative approaches to plant production under extreme conditions relevant to long-term space missions or agriculture on other planets.
Among the key technologies currently used in plant phenotyping are multispectral and hyperspectral imaging, which collect data in different wavelength ranges and allow detailed analysis of plant physiology. These technologies provide critical information on plant health, nutrient content, and other physiological characteristics. In addition, 3D imaging provides a comprehensive view of plant structure and dynamics by creating three-dimensional models that provide insights into plant growth and development. [St21]
Drones and robots collect data in large field trials, providing a high spatial resolution that enables precise monitoring and analysis of plants over large areas. Machine learning, particularly deep learning with neural networks, has proven highly effective in recognizing patterns in complex data sets and identifying stress symptoms. These algorithms can process large amounts of image and sensor data and detect subtle changes and anomalies that indicate stress factors. Therefore, current trends in plant phenotyping involve integrating these technologies to achieve highly detailed phenotyping in fields and greenhouses, supporting the development of new plant varieties and the optimization of agricultural practices. [DCSA19]
In plant and agricultural research, researchers use high-throughput phenotyping systems to support the development of new plant varieties and optimize agricultural practices. These systems enable precise environmental control and detailed phenotyping. High-throughput phenotyping systems are automated technologies that rapidly analyze large volumes of biological samples and capture their phenotypic characteristics. They use imaging techniques, robotics, and data analysis software to measure size, shape, color, and growth characteristics. [Gi22], [Ar18],
In addition to these high-throughput phenotyping systems, the EDEN ISS greenhouse plays

a critical role by focusing on sustainable and automated food cultivation in extreme environments. This greenhouse contributes significantly to the advancement of controlled environment agriculture by integrating advanced technologies for plant health monitoring and stress detection, helping to develop resilient agricultural systems for future space missions and challenging terrestrial conditions. [Ze19]
Despite this progress, several challenges remain. One major issue is the standardization of data collection and processing methods, making comparing results difficult. Many current models are highly data-driven and require large amounts of well-annotated training data, often challenging to obtain in practice. Another obstacle is the generalizability of the models, as researchers often optimize them for specific plant species or conditions, making them difficult to apply to other scenarios. Identifying and analyzing these limitations highlights the need for further research to develop more robust and universally applicable methods.

2.2 Key Studies and Findings

Several fundamental studies have made significant contributions to the detection of plant stress and provide valuable insights for developing and improving methods relevant to the goals of this master's thesis. These goals include developing algorithms for image preprocessing and key feature identification, selecting appropriate machine-learning models for anomaly detection, and conducting experimental tests to validate the hypothesis.
The most significant study on which this work is based is the EDEN ISS study [Ze19]. A central element of this study is the plant health monitoring system, which Wageningen University handled. The system automatically analyzes these images for anomalies and suboptimal performance. Upon detecting abiotic stress, such as inadequate conditions, the system generates warnings. This enables the team to take early countermeasures to optimize plant conditions and minimize stress
Another significant study by Zorn et al. [Zo16] investigates the effects of various abiotic and biotic stress factors on plants. This research demonstrates that detailed phenotyping can precisely identify the causes of abiotic stress and trace them back to specific nutrient deficiencies. Additionally, the handbook for the visual diagnosis of nutritional disorders in plants provides a practical method for assessing abiotic damage on-site and distinguishing it from biotic damage, allowing for targeted nutrient deficiency analysis.
Complementing these studies is the research by Geldhof [Ge21], which focuses on leaf movement in relation to abiotic stress. This method uses a digital inertial measurement unit (IMU) sensor attached to leaves or plant organs to capture real-time angular traits. The

results prove the system can accurately monitor stress-induced leaf movements, facilitating early detection and response to abiotic stress.
Finally, the study by Wesemann [Le20] plays a crucial role in detecting the timing of induced stress. This study analyzes data from wind turbines and demonstrates that change-point detection methods can accurately and automatically identify abnormal events. Over 90% of the signals were correctly classified, highlighting the relevance of these methods for data preprocessing and early threat detection.
The findings from these fundamental studies form the basis for developing and implementing the algorithms used in this thesis to detect anomalies in the EDEN ISS dataset and distinguish healthy from stressed plants. This thesis aims to identify an appropriate machine learning model for anomaly detection and validate it through experimental testing. The experimental tests are conducted to confirm the hypothesis that these new approaches can improve the accuracy of plant stress detection.

2.3 Research Gaps

Detecting plant stress is a crucial research field that is continuously advanced through the use of modern technologies and methods. Despite significant progress in plant phenotyping and stress detection, numerous unresolved questions and challenges remain. This chapter identifies and analyzes existing research gaps and suggests ways to address these gaps through future research efforts.
Despite the widespread use of multispectral and hyperspectral imaging, the potential of RGB imaging in plant stress detection remains largely untapped. RGB images are cost-effective and easier to handle, but their application in stress detection is limited. Accurate extraction of phenotypic traits from RGB images is a complex task requiring advanced algorithms and robust data analysis techniques. Developing efficient methods for feature extraction and selection based on RGB data is a significant research gap that needs to be addressed. Additionally, there is a shortage of extensive datasets specifically focused on abiotic stress factors such as nutrient deficiencies, temperature fluctuations, and water deficits. The availability of such datasets is crucial for the development and validation of new stress detection methods.
The results of various studies on plant stress detection vary significantly due to different imaging techniques and stress detection methods. These inconsistencies make it challenging to compare study outcomes and draw general conclusions. Another significant issue is the need for standardized data collection and processing methods. Different approaches lead to

inconsistent results and hinder the reproducibility of studies. Standardizing these processes is necessary to ensure the reliability and comparability of results.
Current machine learning models have limitations regarding their generalizability to different plant species and environmental conditions. Many models are optimized for specific scenarios and cannot be easily applied to other contexts. Integrating advanced imaging techniques like multispectral and hyperspectral imaging with machine learning models offers great potential for improving plant stress detection. However, more research is needed concerning the optimal methods for combining these technologies to maximize accuracy and efficiency in stress detection.
This chapter has identified and analyzed the key research gaps in plant stress detection. The main gaps were highlighted by the limited use of RGB imaging, challenges in phenotyping, lack of datasets for abiotic stress, inconsistent results, technological and algorithmic limitations, and the need for real-world applications and testing. Addressing these research gaps is essential for advancing the field and supporting sustainable agricultural practices in extreme environments. Future research should focus on closing these gaps to improve the efficiency and accuracy of plant stress detection and enable the practical application of developed methods in real-world scenarios.

3 Background

This chapter provides the essential background for understanding this research. It begins with an overview of the EDEN ISS project, emphasizing its role in advancing sustainable food production in space through CEA systems. Next, it explores plant stress, focusing on abiotic and biotic factors and the methods used to detect and measure these stressors, which are crucial for developing automated plant health monitoring systems. The chapter then covers the basics of image segmentation, which is essential for analyzing plant images from the EDEN ISS project. It also introduces the machine learning approaches to identify patterns and detect plant stress. Finally, it discusses anomaly detection techniques to identify unusual patterns in data, which is vital for monitoring plant health and ensuring optimal growing conditions. Overall, this chapter lays the groundwork for the methodology and analysis in the thesis, providing an overview of key concepts and technologies for detecting abiotic stress in plants using the EDEN ISS dataset.

3.1 EDEN ISS Project

The EDEN ISS project represents a significant step forward in the quest for sustainable food production in space. Technological developments are making long-duration spaceflight possible and increasing the importance of food production in space and on other planets. BLSS can close the air, food, and water loop in a self-sustaining environment, which will be important in space.
The EDEN ISS project has designed, built, tested, placed, installed, and operated a CEA Facility named ISS Mobile Test Facility (MTF) in Antarctica as a first step towards a functional BLSS. The EDEN ISS operation will help understand the food production requirements in space. Because the astronauts cannot be experts in every field and their time is valuable in space, they will be linked to a team of experts on the ground. The limitations make it important to automate the BLSS in the future.
This remote-linked team will have access to all the sensors and data from the MTF and will be responsible for monitoring the plants. Therefore, one focus of the project was on

telemetry, imagery, and remote monitoring, which prepares the way for larger and more efficient space-based agriculture.
Based on this scenario, the data from the MTF has been transmitted via a satellite link to the Mission Control Center (MCC) in Bremen, which will monitor the MTF and the condition of the plants.
To automate the monitoring of the Facility, plant health imaging systems play a key role in the plant growth environment. These systems provide valuable biological feedback data, enabling fine-tuning environmental conditions for optimal plant growth and can send warnings when biotic or abiotic stress will be detected. [Ze19]

In detail, the MTF consists of two 20ft (approximately 6m) containers placed near the Neumayer Station III (NMIII), a research facility from the Alfred-Wegener-Institut (AWI) for Polar and Marine Research. One container, the service section (SES), contains most of the technical Systems, while in the other container, the Future Exploration Greenhouse (FEG), the different plants will be grown. [Ze19]
To be independent of the environment, the MTF needs to replace the environment in which plants need to grow with different systems. The replacements include the obvious elements like air, light, nutrients, thermal, and oxygen. Because microbiological contamination in space can be a great danger for the crew, plants, materials, and environments, there was also decontamination and a bio-detection system in the CEA. Further systems were necessary for controlling, monitoring, and communicating with the base station. [Sc26]

The monitoring system consisted of about 17 HD cameras for RGB images and cameras that collected multi-wavelength images. Each camera took one image per day and sent it over the satellite connection to the NMIII to the DLR control station and then to the different partners, who were responsible for the specific tasks [Ze19]. These systems must be configured according to the other systems and specific plants. As an example of the dependencies, to capture RGB images, the light system (LS) for the plants has a specific mode, which changes the light spectrum so the monitoring system can capture and save the Images. Different plants need different light wavelengths for optimal growth, and the plant species itself has to be selected based on the needs in space and the CEA [Za20].
In Figure 3.1 shows an overview of the FEG, which includes the position from the cameras, the racks, and the tray where the plants have been grown.

At the time of this thesis, the MTF had to be shipped back to the DLR in Bremen, where

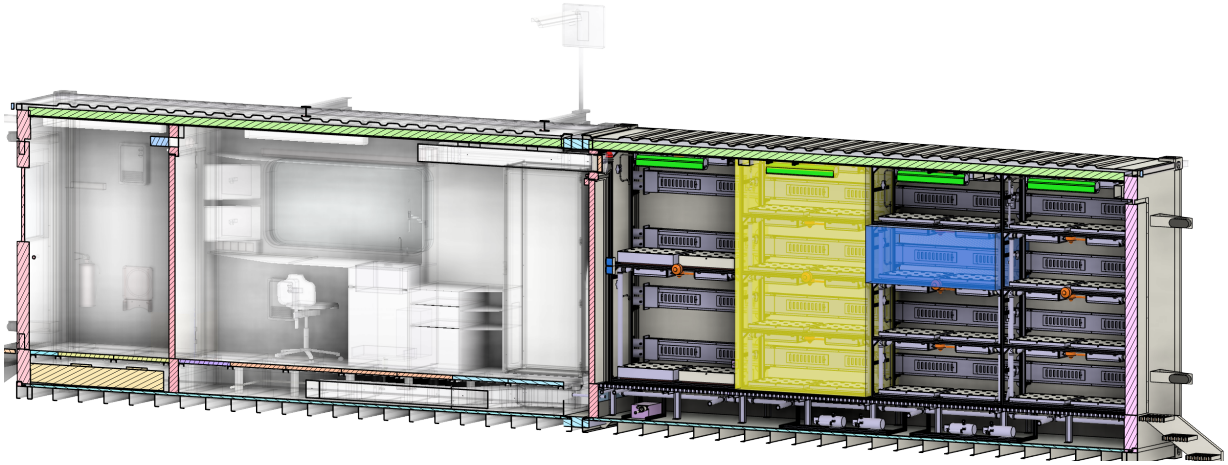

Figure 3.1: Cross-section of the MTF with the FEG section on the right side containing racks and trays for growing plants

maintenance work and further development based on the knowledge from the last years are being done. The MTF will be transported to the EDEN LUNA test center in Cologne and used to train moon astronauts. They will practice growing plants and familiarize themselves with the technology in the building. The EDEN LAB is also placed in Bremen and has systems similar to the EDEN ISS FEG [Sc22]. Following the EDEN ISS project, the EDEN NEXT GEN project takes place and takes a step toward getting a CEA in space. This project is a design study that focuses on building a CEA to fit in a space rocket and having the redundancy systems it needs for space. This project will also modify the systems based on the knowledge from the EDEN ISS project. Based on the humans' positive psychological response and fresh vegetables, an idea for building a CEA inside the NMIII was developed. [Sc22]

3.2 Plant Stress

This section explains the basics of plant stress and then examines the causes and how they affect the plant. It starts with a basic overview of the categories of plant stress and then describes how to identify the cause of plant stress and the visual characteristics of that stress on the plant. An overview of plant resistance is given, including when it is too late for recovery and when the plant is acutely damaged. It also describes how to measure stress in plants, which indices can be used, and which sensors can detect stress in plants at what stage.

3.2.1 Overview of Plant Stress

Plant stress is already significantly impacting agricultural land and will become even more important in the future due to climate change. Plants depend on several critical elements to maintain and develop their growth. These include carbon, which serves as the primary component for photosynthetic processes; light, which is essential for photosynthesis; nutrients, which are essential for growth and metabolism; and water, which is fundamental for hydration and nutrient transport.
Plant stress can be divided into two groups, as shown in Table 3.1, which includes further subgroups. On the one hand, **abiotic stress** refers to non-living and physical elements in an ecosystem more corresponding to the plant's environment. This covers stress from insufficient or too much water, light, nutrients, air, and temperature. On the other hand, **biotic stress** refers to living elements in the ecosystem, which include insects, microorganisms, and herbivores. Both stresses can be connected, so a plant needs optimal growth conditions to mitigate increased susceptibility to pathogens and other biotic stresses.

When recognizing biotic and abiotic stress, it is essential to remember that not only one stress factor can affect a plant. Most of the time, several stress factors affect the plant simultaneously; for example, in dry, sunny, and warm summer periods, often a combination of heat, water deficiency, and high light will affect the plant. A primary symptom can weaken a plant, and a secondary symptom, such as biotic stress, can infect the plant. It is also possible that multiple abiotic and multiple biotic stresses can cause a plant's visual expression. Tracing back to the course can be deficient and may result in more than one unique result. The impact of sub-optimal elements on plants underscores their vulnerability. Natural and human-induced stressors, whether abiotic or biotic, can influence vegetation, leading to reversible, irreversible, or acute damage, thereby shaping growth and developmental dynamics. While biotic stresses directly threaten plants by infecting or consuming them, several approaches mitigate biotic stresses. Preventive measures, which include adherence to sound agronomic practices and regular hygiene protocols, are fundamental strategies. Biological control, which relies on natural enemies or specific pathogens, is a promising avenue for mitigating pests. At the same time, using plant strengtheners that selectively enhance plant immunity and the targeted selection of resistant cultivars can reduce susceptibility to biotic stressors. Complementary cultural practices, including effective crop rotation and soil conservation techniques, are recommended to reduce the risk of biotic stress. Chemical pesticides should be used as a last resort and with extreme caution, given their potential adverse

Table 3.1: Various stress factors encountered by plants [BG21]

Type of stress			
Natural	Abiotic	Light	High irradiance—photoinhibition and photooxidation
			Low irradiance
		Temperature	High/heat
			Low (chilling/frost)
		Drought	
		Flood	
		Mineral deficiency	
	Biotic	Insects	
		Viruses	
		Fungi	
		Bacteria	

effects on the environment and human health. The optimal approach to sustainable biotic stress management in agricultural settings often emphasizes the synergistic integration of different methods.

3.2.2 Abiotic Plant Stress

Unlike biotic stress, abiotic stress can be prevented by adapting the plant's nutrition. Abiotic stress can be divided into different stress factors, which are the critical elements listed above that a plant needs to maintain and develop its growth.

Temperature Stress: Every plant species has a different optimum temperature range for best survival and a different minimum and maximum threshold. Temperature stress can have a significant impact on plants, whether the temperature is too high or too low.

Low Temperatures Stress: Low temperatures stress has several types of damage, including desiccation, chilling, and frostbite, the severity of which depends on the duration and intensity of the cold. Plant resistance to cold injury varies from species to species. Some plants suffer chilling injury at temperatures as high as 10-15 degrees Celsius, while others are only affected at 0-5 degrees Celsius.[BG21] Still, other plants develop frost tolerance, while others, such as hardy or woody plants, are highly immune to cold injury. The effects of cold injury can be diverse, including changes in membrane structure and composition, reduced protoplast flux, altered respiration and photosynthesis, abnormal metabolite production, slowed growth, leaf curling, necrosis, stem decline, abnormal fruit ripening, and altered reproduc-

tive behavior. Plants adapt to cold injury by altering various biochemical and physiological processes.

High-Temperature Stress: Due to increasing changes in global mean temperature and light conditions, high temperatures stress is becoming more important. Climate change can reduce the cultivable area for some species by 63-100%.[BG21] Similar to low temperatures, high temperatures can be further categorized into responses to excessive, moderate, and low temperatures. High temperatures or heat stress damage plants, reduce growth and development, scorch leaves and fruit, and cause sunburn. As with low temperature, there are different threshold limits from species to species.

Light Stress: Light is an important factor in the assimilation of CO2 through photosynthesis. However, there are limits to the amount of light a plant can receive, and each plant species is different and has different limits to the amount of light it can receive. To avoid light stress, plants change the angle of their leaves, curl their shoots, densely cover the upper surface of their leaves with trichomes, hair-like structures with various crucial functions for plant survival, and thicken their cell walls.

Water Stress: Non-woody plants are highly dependent on water, which makes up approximately 80-90% of their composition and is essential for maintaining all metabolic processes. Water plays a central role in several physiological functions in plants. Its availability can become a significant stress factor if it is limited or not readily accessible to the roots, especially at high transpiration rates. Both water deficits and surpluses, such as flooding, can lead to water stress.

In the case of flooding, the excess water in the soil reduces oxygen availability, limiting root respiration and overall plant health. This phenomenon alters the dynamics of cellular processes within plants. In response to the water deficit, the water potential within the cells decreases, causing stomatal, tiny openings on the surfaces of leaves and stems that regulate gas exchange and closure. Plants typically exhibit hydro passive stomatal closure to minimize transpiration losses. Consequently, this closure restricts gas exchange, reduces transpiration and photosynthesis rates, interferes with mineral nutrient uptake, and disrupts ion and homeostasis balances.
Under water stress conditions, plants adapt by adjusting their root-to-shoot ratio, often resulting in inhibited growth and reproduction. In addition, the altered growth pattern of

the plant may manifest itself in attempts to expand or spread differently. Prolonged periods of waterlogged soil due to flooding or excessive irrigation further exacerbate plant stress. The accumulation of water limits the availability of oxygen to the roots, resulting in potential damage depending on the adaptability of the plant species and the soil conditions.
The extent of damage caused by water stress also depends on various factors such as plant species, developmental stage, genotype, and the magnitude and duration of water stress. It underscores the complex interplay between environmental conditions and plant biology and highlights the critical role of water in shaping plant growth, development, and resilience.
Nutrien and Salinity Stress: Other stress factors are nutrients and salinity. Too much or too little concentration of nutrients or salinity can be harmful depending on the plant's symptoms, intensity, and duration. The following remark in the Subsection 3.2.2 will be shown here to highlight the importance of nutrients.

> "Without minerals, no life is possible for plants, animals, and humans! An inadequate or unbalanced mineral balance must, therefore, inevitably lead to complaints, reduced performance, and illnesses in plants, animals, and humans." [Transl. by the author.] [Zo16]

This quote emphasizes the need for plants to have a balanced nutrient and salinity concentration. It also clarifies the need by saying that animals and humans need a balanced mineral concentration for a healthy life.
To achieve balance, we have to measure concentration or use an indicator and then add or reduce nutrients. As in the quotation described, plants are rough, similar to humans or animals. In this case, when a human feels ill, we go to a doctor, who then tries to identify the problem by asking questions and performing tests. Similarly, it is possible to reduce the issues from the plants to specific nutrients by checking different indicators from the plants, like in the Figure 8.1 in the appendix.

To identify the cause of the stress, a good and detailed phenotyping of the plant is necessary. The pathway analysis to identify which specific nutrients are the cause of the symptoms is based on different characteristics, such as where and on which part of the plant the stress symptoms first appear, whether the symptoms are at the beginning or at an advanced stage and whether secondary infections by microorganisms are part of the symptoms. Moreover, it considers whether the environmental factors before and during the development of nutritional damage are to be classified as favorable or unfavorable.

In addition to the outward appearance of plant stress, whether caused by abiotic or biotic factors, indices and metrics play a critical role in the comparative analysis of plants. These are used not only to measure the extent of stress but also to assess the vitality and health of the plants. These metrics are based on various remote sensing techniques that can capture the spectral signature of plants, including satellite and drone imagery.

The Normalized Difference Vegetation Index (NDVI) is one of the most prominent and widely used indices. It uses the near-infrared (NIR) and red (R) spectra to provide information on chlorophyll activity and, thus, vegetation health. By calculating the ratio of reflected radiation in the NIR and R spectral regions, NDVI can provide valuable insight into biomass production and the overall physiological condition of plants. [Rh11] The formula for NDVI is:

$$\text{NDVI} = \frac{\text{NIR} - R}{\text{NIR} + R}$$

where NIR represents the near-infrared channel, and R represents the red channel.
In addition to the NDVI, more specific indices have been developed to measure different aspects of plant health. The Green Leaf Index (GLI) determines the grazing impact on wheat and is sensitive to green leaves or stems. [Bh20] The formula for GLI is:

$$\text{GLI} = \frac{2G - R - B}{2G + R + B}$$

where G represents the green channel, R represents the red channel, and B represents the blue channel. A positive value indicates the presence of green leaves or stems, while a negative value represents soil or nonliving matter.
Similarly, the Visible Atmospherically Resistant Index (VARI) aims to provide resilient information on vegetation health using the ratio of green, red, and blue light to atmospheric disturbances. [BEK19] The formula for VARI is:

$$\text{VARI} = \frac{G - R}{G + R - B}$$

where G represents the green channel, R represents the red channel, and B represents the blue channel. This index minimizes atmospheric effects and can estimate vegetation fraction with an error of less than ten percent.

A promising approach to assessing plant health is using UV spectrometry, which measures fluorescence in plants. This technique can detect subtle changes in pigment composition and

physiological processes such as photosynthesis, making it an important tool for diagnosing plant health.
In addition, combined approaches such as multispectral and hyperspectral cameras are being used to gain a more comprehensive understanding of plant health. These advanced technologies capture a wide range of spectral bands and make it possible to extract detailed information about the physiological state of plants. However, despite their potential, such technologies often require significant financial investment and specific expertise to apply and interpret.

3.2.3 Plant Stress Resistance

Plants are exposed to low abiotic or biotic stress; they often activate various physiological and molecular mechanisms to increase their resistance or tolerance to those stressors. This phenomenon is known as priming, where plants, after an initial exposure to a mild stress, become more resilient to subsequent stress events through enhanced and faster activation of defense responses, or acclimation. When plants experience mild stress, they can change at the cellular, biochemical, and molecular levels, which prepares them to better cope with future stress events. These changes can include alterations in gene expression, production of stress-related proteins, accumulation of antioxidants, and adjustments in hormone levels. For example, exposure to mild drought stress can produce osmoprotectants, such as proline or sugars, which assist the plant in maintaining cellular water balance during future drought conditions. Similarly, encountering low levels of pathogen attack can stimulate the activation of defense genes and the production of antimicrobial compounds, thereby enhancing the plant's ability to resist subsequent pathogen invasions.
Figure 3.2 illustrates the average progression of stress resistance in plants, categorizing plant stress into eustress and distress. Eustress positively impacts plants by enhancing their robustness against future stressors, while distress negatively affects them, potentially causing damage.
The diagram shows different time phases within these eustress and distress areas after the onset of stress. Under low-stress conditions (shown by the thick solid line), the successive phases lead to the hardening and stabilization of the plant. However, under severe or additional stress conditions (shown by the dashed lines), these phases can lead to damage and possibly death of the plant. The numbers on the curves correspond to specific scenarios: (1) severe stress leading to acute damage and death of the plant, (2) minor stress leading to hardening and stabilization, with debonding occurring after the stress is removed, (3)

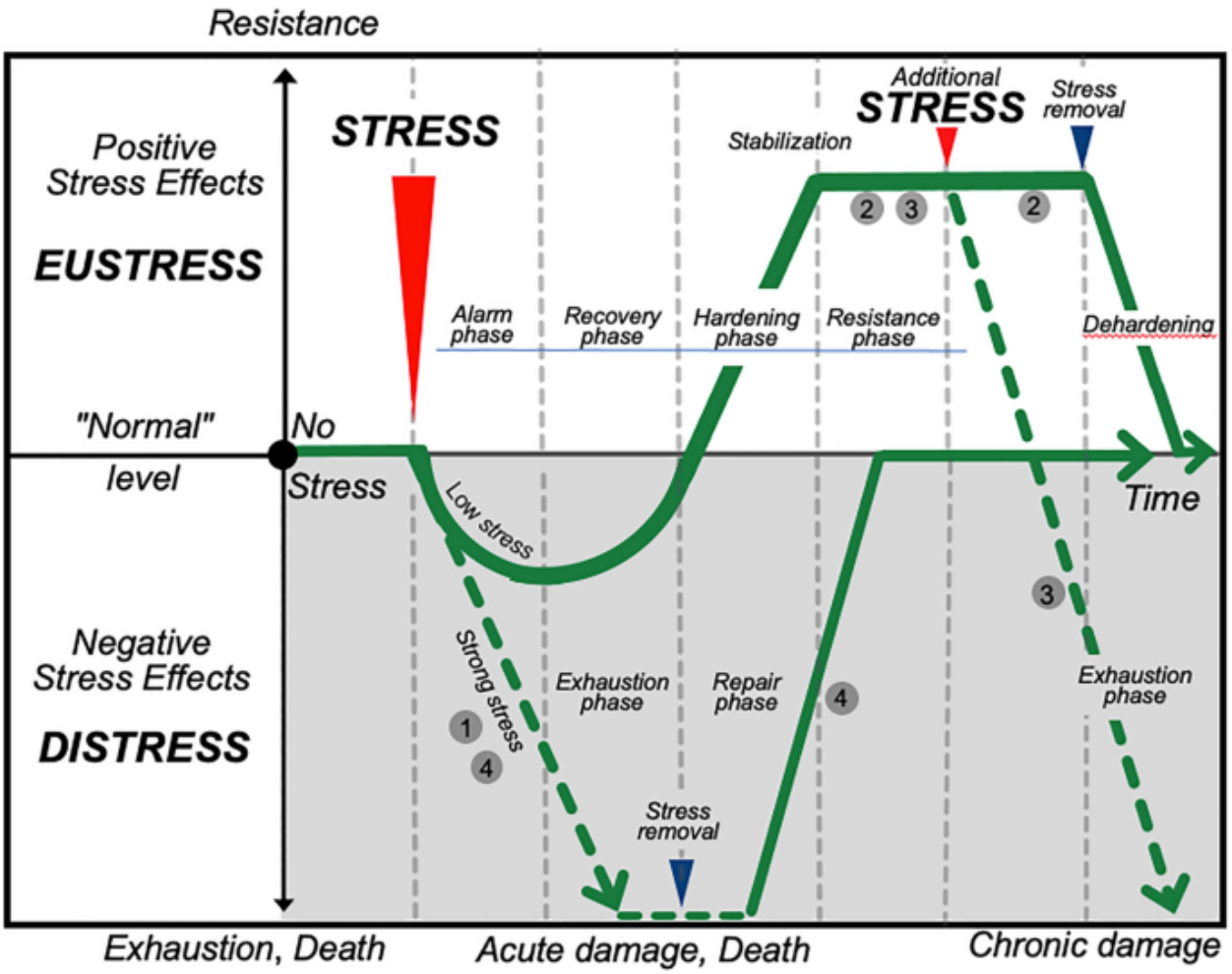

Figure 3.2: Positive and negative of stress on a plant over time [GSL22]

additional stress leading to chronic damage, and (4) removal of damage after severe stress returning the system to its initial state (represented by the thin solid line). [GSL22] Different plant species have different stress resistance and recovery phases. This diagram emphasizes the importance of early detection of stress. Early detection and removal of stress give the plant enough time to recover. Conversely, failure to detect stress early can lead to acute damage or death. [BSA09].

3.3 Image Segmentation

This section provides a basic understanding of image segmentation, a core concept in computer vision crucial for extracting meaningful information from visual data. By exploring the fundamental principles and methodologies of image segmentation, readers will be equipped

with the essential knowledge to understand image analysis and interpretation in computer vision applications. This section will also touch on related tools like histograms and color spaces, which play a role in the segmentation process.
Histograms are essential tools for understanding the distribution of pixel intensities within an image, providing insights into exposure, contrast, color distribution, and potential image defects. They are widely used in image enhancement, segmentation, and classification. Color spaces, such as RGB, HSV, CMYK, and LAB, are different methods of representing and organizing color based on application requirements [SQP02]. Each color space has advantages and is suited to specific applications like digital displays, image processing, printing, and color measurement.

Image segmentation is crucial in image processing and computer vision, allowing images to be divided into semantically meaningful regions or objects. Various methods and techniques for image segmentation are explored based on the concepts of discontinuity and similarity [Go08]. Image segmentation often relies on two fundamental principles: discontinuity and similarity. Discontinuity refers to abrupt changes in the intensity values of an image, typically caused by edges or boundaries between objects. Similarity, on the other hand, refers to neighboring pixels having similar properties such as color, texture, or intensity.
A standard method for capturing discontinuities is edge-based segmentation, where edges or contours in the image are identified. The Canny edge detection is an example of an algorithm used for this purpose [KB09].
In contrast to edge-based segmentation, region-based segmentation groups pixels based on similarity. Methods such as clustering or generating superpixels are often used to group similar pixels. Combining edge-based and region-based approaches often leads to more robust segmentation results. For example, edge information can be used to guide or enhance the region formation process [Lu17].
Image segmentation is an essential step in image processing and computer vision. Various techniques can be applied to divide images into meaningful segments by combining concepts of discontinuity and similarity. The choice of the appropriate method depends on the image's specific characteristics and the segmentation task's requirements. Careful selection and combination of these methods can lead to precise and robust segmentation results applicable in a variety of domains, including medical imaging, robotics, surveillance, and autonomous driving.

3.4 Machine Learning

Machine learning is a pivotal area of artificial intelligence, aiming to identify patterns and relationships within data to facilitate predictions or decision-making processes. The selection of an appropriate machine learning approach is contingent upon the nature of the available data and the desired outcomes. The primary categories include supervised learning, unsupervised learning, and semi-supervised learning.

3.4.1 Supervised Learning

Supervised learning involves training a model with labeled data, where each training instance comprises an input vector and the corresponding desired output vector. The objective of the model is to discern the relationship between inputs and outputs to accurately predict the outputs for new, unseen inputs.
A paradigmatic example of supervised learning is email spam filtering. In this scenario, the model is trained using a substantial dataset of emails labeled as either "spam" or "non-spam". The model learns to recognize specific patterns and features indicative of spam, thereby enabling it to classify new incoming emails appropriately. The quality of the training data is paramount; more precise and comprehensive labeled data enhance the model's learning and predictive capabilities [Pa12].
In supervised learning, various neural network architectures are employed, particularly when handling large and complex datasets. Convolutional Neural Networks (CNNs), for instance, are designed for processing data with a grid-like topology, such as images. CNNs utilize convolutional and pooling layers to extract and condense features from input data, proving especially effective in image recognition and classification tasks, such as identifying tumors in medical imaging [Da19].

3.4.2 Unsupervised Learning

Unsupervised learning entails the use of models to analyze unlabeled data, with the goal of uncovering hidden patterns or structures. Unlike supervised learning, there are no predefined outputs for the model to learn.
An illustrative example of unsupervised learning is customer segmentation in marketing. Here, customer data, including purchasing behavior and demographic information, is analyzed to identify groups of similar customers. These segments can subsequently be leveraged for targeted marketing campaigns. The quality of the data is critical, as only meaningful

and well-structured data can reveal reliable patterns and clusters [Ga23]. Autoencoders are a type of neural network frequently employed in unsupervised learning. These networks are trained to compress high-dimensional data into a lower-dimensional form (encoding) and then reconstruct it (decoding). Applications of autoencoders include dimensionality reduction, image denoising, and generative modeling [ZIE17].

3.4.3 Semi-supervised Learning

Semi-supervised learning integrates elements of both supervised and unsupervised learning by utilizing a combination of labeled and unlabeled data. This approach is particularly advantageous when there is a limited amount of labeled data but a large volume of unlabeled data available.
An exemplary application of semi-supervised learning is speech recognition. A model can be trained with a small set of labeled speech recordings (words or sentences) and a large set of unlabeled speech recordings. The labeled data helps the model learn the fundamental structure of the language, while the unlabeled data further refines this structure, improving recognition accuracy. The representativeness and high quality of the labeled data are crucial to providing the model with a robust foundation [Ma09].
Recurrent Neural Networks (RNNs), including Long Short-Term Memory Networks (LSTMs), are particularly effective in semi-supervised learning contexts, especially for sequential data. RNNs are adept at processing sequences and modeling temporal dependencies, making them suitable for tasks such as speech recognition and machine translation. LSTMs, in particular, are useful for handling data with long-term dependencies [SNL19].

3.5 Anomaly detection

Anomaly detection is an essential area of data analysis that focuses on identifying unusual patterns or deviations in datasets that deviate from expected behavior. These anomalies can indicate significant events such as fraud, technical failures, or health issues. The applications of anomaly detection are diverse. In finance, it is used to detect fraudulent transactions to minimize losses from criminal activities. For example, an unusually large transfer from a rarely used account might be marked as potentially fraudulent. In medicine, it enables early detection of diseases by analyzing patient data and identifying abnormal patterns in biological signals. For instance, detecting an unusual heart rhythm in a patient could indicate a serious cardiac problem. In industry, it monitors technical systems to identify

malfunctions or failures early, such as detecting an unusual vibration pattern in a machine that could indicate an impending failure. In cybersecurity, anomaly detection plays a crucial role in identifying unusual activities in networks, such as a sudden increase in traffic to an unusual IP address.

Anomaly detection is based on identifying data points or patterns that significantly deviate from the rest of the dataset. These deviations, or anomalies, can be attributed to various causes such as errors, fraud, or rare events. There are three main categories of anomalies: point anomalies, contextual anomalies, and collective anomalies. Point anomalies are individual data points that significantly deviate from the majority of the data. An example would be an unusually high transfer in a bank account. Contextual anomalies occur only in a specific context. For example, a sudden increase in heart rate during sleep would be considered anomalous compared to normal sleep data. Collective anomalies involve groups of data points that together form an anomalous pattern, even if individual points may not appear unusual. An example would be unusual purchasing behavior within a certain period, such as a large number of high-value purchases in quick succession. [HC15], [Ar16]

Anomaly detection methods can be broadly classified into supervised, unsupervised, and semi-supervised methods based on the availability of labeled data. Supervised methods require labeled training data to create models that distinguish between normal and anomalous data points. Classification-based methods such as decision trees and neural networks are commonly used. For instance, a decision tree can detect fraudulent credit card transactions, while regression techniques can predict normal behavior patterns and identify deviations, such as predicting normal stock prices and detecting unusual price movements.

Unsupervised methods do not require labeled data and rely on the structure of the data to identify anomalies. Cluster-based methods group data points and identify those that do not belong to any group. For example, k-means clustering can detect anomalies in sensor data from an industrial monitoring system. Density-based methods like DBSCAN (Density-Based Spatial Clustering of Applications with Noise) and Local Outlier Factor (LOF) detect anomalies based on the density of their neighborhood, such as identifying unusual network accesses based on access pattern density [Al21].

Semi-supervised methods use both labeled and unlabeled data. A well-known technique is the One-Class SVM (Support Vector Machine), which learns a model of normal behavior from the labeled data and identifies anomalies in the unlabeled data. An example of applying One-Class SVM is detecting machine faults in a production line, where the model is trained on data from normal operating conditions and detects anomalies in real-time. Novelty detection with Local Outlier Factor can also be considered semi-supervised when it leverages a

combination of labeled normal data and unlabeled data to improve the detection of new or rare events. This method is particularly useful in scenarios where a comprehensive labeled dataset is not available, but sufficient labeled examples of normal behavior exist to guide the detection process.

4 Datasets

This chapter describes and explains the datasets used in this thesis. First, the EDEN ISS dataset, which consists of the three species selected for this thesis and serves as the basis for stress detection, is presented. Second, the Plant Phenotyping dataset, chosen to compare segmentation algorithms, is discussed.

4.1 EDEN ISS Dataset

The EDEN ISS dataset consists of data recorded during the EDEN ISS project Section 3.1, primarily focusing on RGB images of plants taken by cameras inside the FEG. In addition to the RGB data, other sensors, such as temperature and humidity sensors, as well as multi-wavelength images, were recorded during the project. However, this dataset will deal with the RGB images and the three species: dragoon lettuce, kohlrabi, and cucumber.

4.1.1 Description of Dataset

The collected original data was transmitted via FTP to the NMIII station and then over a satellite connection to the MCC in Bremen, where it was stored. A total of 17 HD cameras captured the RGB images in the dataset. These cameras are positioned above the plant tray, capturing daily images of various plant species selected based on specific criteria.[Ze19] The dataset is divided into 14 species, and some sample images are shown in the Figure 4.1.
The advanced imaging system in the EDEN ISS employs cameras in various positions to capture these images. This imaging system integrates HD HIKVISION DS-2CD2542F-I cameras into the growth system, which can capture both top-view and lateral images. Seven visual HD cameras are installed on the ceiling of the first to third levels of the rack, with two cameras per level/one for each tray. One camera is used to cover the entire upper level. These cameras also point downward towards the trays, ensuring detailed top-view imaging of the growing plants.
The second position is where eight visual HD cameras are positioned along the corridor, with

(a) (b) (c)

Figure 4.1: Example images from the dataset showing planting trays with (a) dragoon lettuce, (b) kohlrabi, and (c) cucumber.

two cameras per rack mounted on the rack structure pointing at the opposite rack. These cameras capture lateral-view images, offering a different perspective on plant growth and health. To conclude, an overview of the tray's structure is shown in the Figure 4.2.

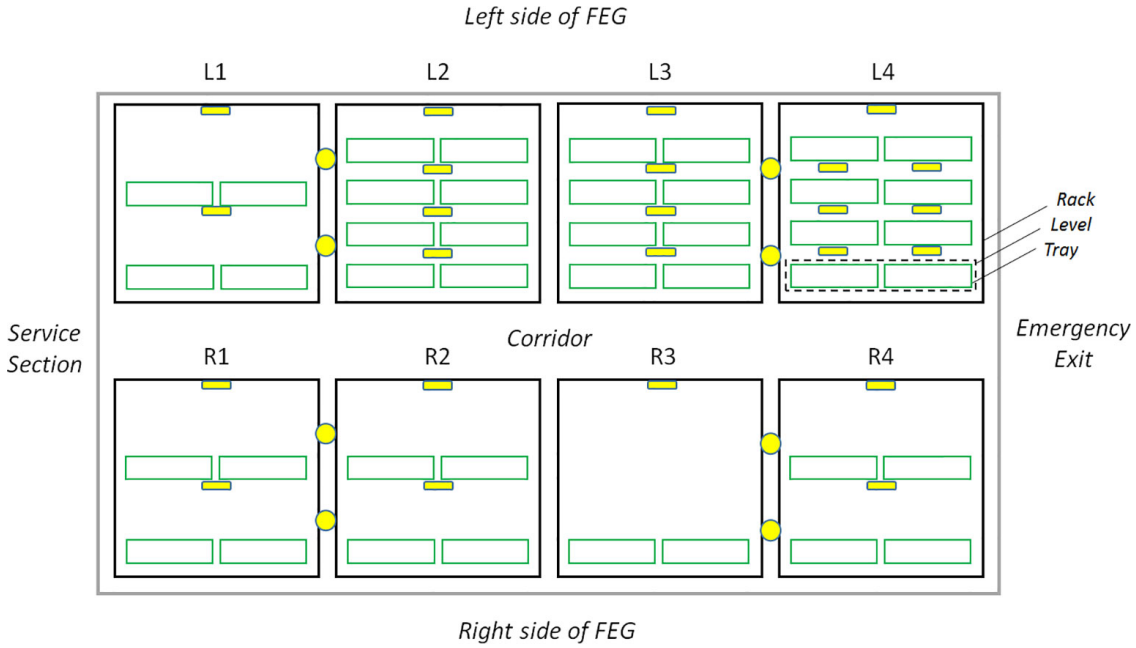

Figure 4.2: Schematic representation of the racks (black), trays (green), and camera positions (yellow) in the greenhouse [Ze19]

The yellow circles represent the side view cameras, and the yellow squares represent the top view cameras. On each side of the container are four plant growth racks (black outlines) labeled L1 through L4 for the left side and R1 through R4 for the right side. Each rack is divided into four growth levels (green outlines) consisting of two plant growth trays[Ze19].

4.1.2 Structure of the Dataset

The dataset primarily consists of image files and associated metadata. The images are organized in folders based on time series. The plants are identifiable by the names of the trays and can be sorted using a configuration file.
Example of the structure:

```
/dataset
  /lettuce_1
    HDCam_L2-2C_20200626_2358.jpeg
    HDCam_L2-2C_20200627_2358.jpeg
    ...
  /lettuce_2
    HDCam_L2-2C_20180509_2358.jpeg
    HDCam_L2-2C_20180510_2358.jpeg
    ...
  config_file.json
```

The images are saved with their original names. The naming convention for the images follows a structured format that includes the camera position, tray identification, and timestamp. For example, in the filename `HDCam_R1-2C_20200112_2358.jpeg`, "HDCam" indicates the camera type, "R1-2C" specifies the tray position, and "20200112_2358" denotes the timestamp (year, month, day, hour, and minute). This naming convention ensures that each image is uniquely identifiable and traceable to its specific context within the dataset.
A folder structure was created to identify the various images of the tray's growth, along with a labeling file. A configuration file was incorporated to further enhance the dataset. This file provides crucial information about the trays, the start and end of the time series, and the plant species involved. However, it is important to note that the labeling process was conducted by non-experts, which introduces the possibility of incorrect classification of plant species. The configuration file `config_file.json` contains the following information:

```
{
    "start_image": {
        "filename": "HDCam_R1-2C_20200112_2358.jpeg",
        "timestamp": "2020-01-12T23:58:00"
    },
    "end_image": {
```

```
        "filename": "HDCam_R1-2C_20200225_2358.jpeg",
        "timestamp": "2020-02-25T23:58:00"
    },
    "alignment": "Left",
    "species": "Kohlrabi",
    "split_line_x": 2220
}
```


The configuration file stores the names of the first and last images of the time series, specifies the species, and details the location within the tray. The `split_line_x` coordinate divides the trays for species included in this study.

4.1.3 Data Quality and Preprocessing

To ensure the integrity and relevance of our dataset, images that did not contain plants or were taken during the germination phase were excluded. Additionally, time series data from shelves without plants were removed. During the recordings, the lighting system of the EDEN ISS was modified to a specific spectrum, resulting in some images being blurry or obscured by overgrown plants. These images were retained in the dataset to preserve the traceability of any missing images and ensure comprehensive documentation. Figure Figure 4.3 presents examples of problematic images within the dataset.

(a) (b) (c) (d)

Figure 4.3: Examples of problematic images: (a) Outlier with poor image quality. (b) Image with incorrect lighting. (c) Image obscured by overgrown plants. (d) Blurry image.

The dataset is available upon request. A publication of the dataset is also planned for future dissemination.

4.2 Plant Phenotyping Dataset

The Plant Phenotyping Datasets, version 1.0, released on 4 December 2015, are a comprehensive collection of benchmark datasets to enhance research in plant phenotyping. The data includes ground truth segmentations, annotations, and metadata, facilitating the development and evaluation of computer vision and machine learning algorithms. [Mi15]

4.2.1 Description of Dataset

These datasets are designed for various computer vision tasks, including plant detection and localization, plant segmentation, leaf detection, localization, counting, leaf segmentation, leaf tracking, boundary estimation for multi-instance segmentation, and classification and regression of mutants and treatments. These datasets are valuable for scientists in related fields and general computer vision researchers. Utilizing these datasets helps advance state-of-the-art phenotyping and contributes to global agricultural improvements. In this context, we will focus only on the plant segmentation aspect of the work.

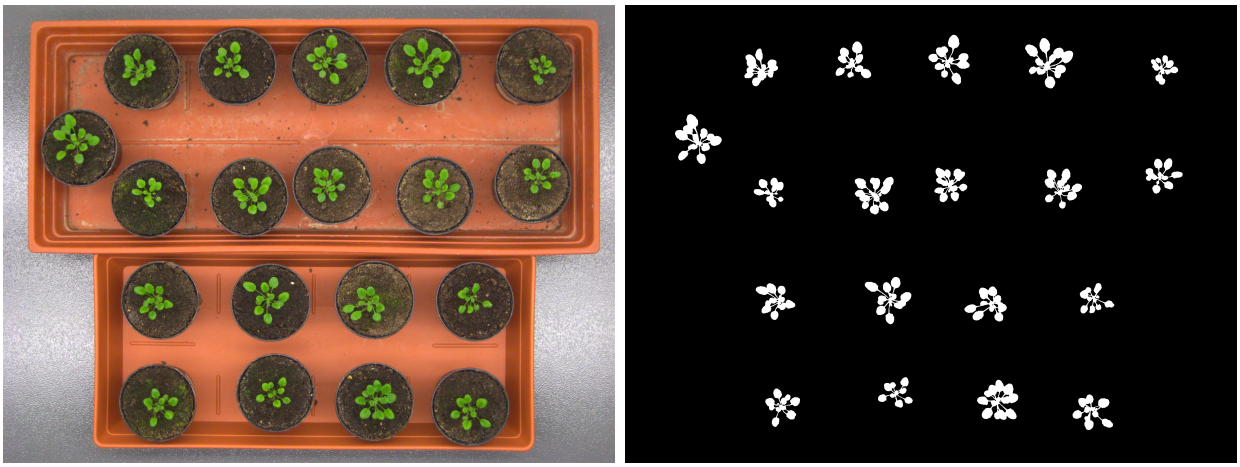

(a) (b)

Figure 4.4: Example of (a) an RGB image of plants and (b) the corresponding mask

The images in Figure 4.4 include the RGB image of multiple plants and its corresponding mask. Using an accompanying CSV file within the dataset, various images can be cropped and compared with the results produced by segmentation methods. Figure 4.5 presents several examples of these cropped images. The dataset contains 19 different plants, with images captured 16 times over a period. Examples from different days are shown in Figure 4.6 and demonstrate the differences over time.

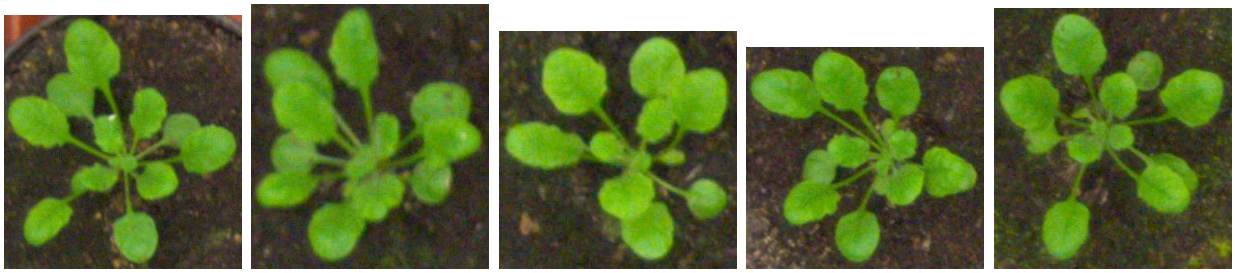

Figure 4.5: Examples of separate images for plants cropped from an image of an entire tray of plants

(a) day 1 (b) day 4 (c) day 8 (d) day 11 (e) day 13 (f) day 16

Figure 4.6: Example images of a single plant in a tray over multiple days

4.2.2 Structure of the Dataset

The image data in the Plant Phenotyping Datasets are divided into three main groups: the first group, "Plant," consists of color images of single plants with annotations such as leaf segmentation masks, leaf bounding boxes, leaf centers, leaf boundaries, and metadata. The second group, "Stacks," comprises time series of single plant images with time-consistent annotations, including leaf segmentation masks and leaf bounding boxes. The third group, "Tray," contains color images of trays with multiple plants and annotations such as plant segmentation masks and bounding boxes. Focusing on the plant segmentation task, the relevant dataset files are organized as follows:

- Ara2012:
  - Image Files: Tray/Ara2012/*_rgb.png (16 files)
  - Segmentation Masks: Tray/Ara2012/*_fg.png (16 files)

These files contain color images of trays with multiple plants and corresponding foreground segmentation masks. The segmentation masks are binary images where the foreground plants are distinguished from the background.

5 Methodology

This chapter explains the different methods used in this thesis. This includes comparing different segmentation techniques to separate the foreground plants from the background to ensure accurate and reliable analysis. The chapter then discusses the methods used to crop the images, followed by a detailed explanation of the techniques used to extract features from the images. These features, which are indicative of plant stress, are identified using statistical methods to determine the significant indicators. Finally, the method for detecting the time stamp when a plant first shows stress is explained.

5.1 Overall Concept

The proposed Plant Stress Detection System is visualized in Figure 5.1. It uses image data from an external Image Database, in this case, the time series data from the EDEN ISS. The system then classifies the plants, detects the time when the plants become stressed, and sends this information to the warning system.
The system itself is divided into three containers, each dependent on the results from the previous container.

1. Preprocessing: The first container is responsible for pre-processing the data. This container identifies the different trays containing the plants and detects the position and contour of the seedlings. Based on this information, the container crops out individual plants and segments the images to remove the background. In another approach, multiple plants are cropped at once and then segmented similarly to the previous method.

2. Feature Extraction: The purpose of this container is to extract features that serve as potential indicators of plant stress. Once extracted, these features are normalized and equalized in length to ensure they are the same length, which makes them easier to analyze.

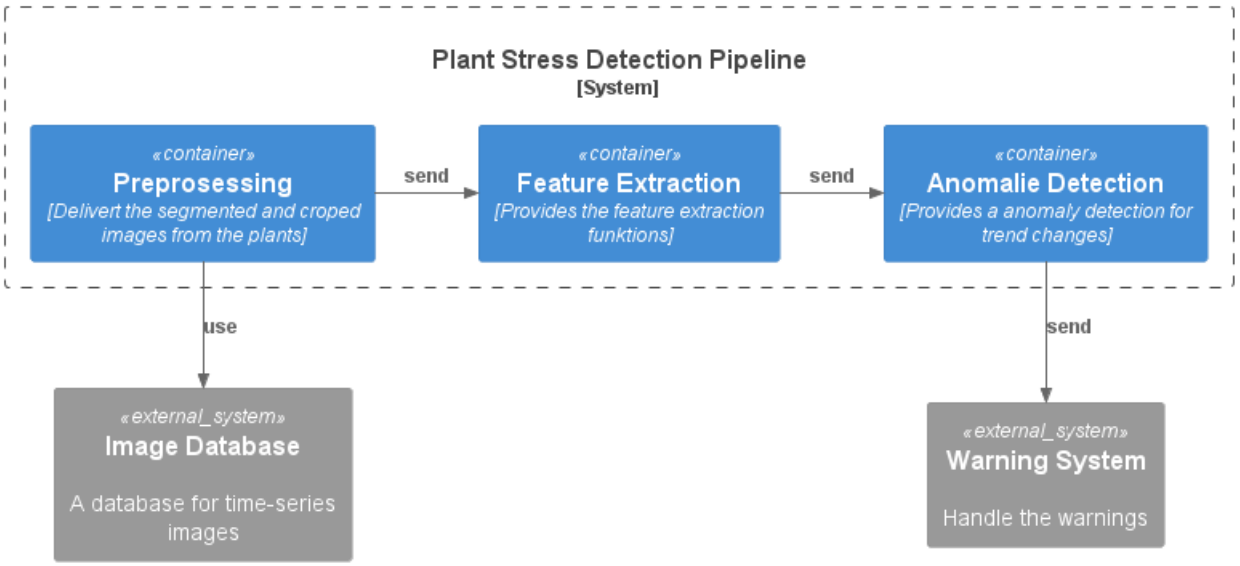

Figure 5.1: Container diagram showing a high-level overview of the proposed Plant Stress Detection System

3. Anomaly Detection: The final container detects turning points in the various trends and classifies the time series as healthy or unhealthy. First, an average time series is calculated from the healthy plants to serve as a baseline for model training. This model involves segment analysis of the time series to accurately identify the time of change. Based on the detection of these change points, the classification of plants as healthy or stressed is performed.

The structured design of the three containers minimizes data flow and dependencies, with each container focusing on a primary task. This modular approach makes it easier to test and compare the containers. The methods used in these three containers are described in more detail in the following sections.

5.2 Preprocessing

This container and its components are fundamental to this work, as they influence all subsequent results and serve as the basis for further processing. The first and second components are designed to automate the process for each plant, reducing the need for manual tasks. While manually cropping trays and plants may initially seem faster and more accurate, the automated approach can save significant work hours in the future and represents a first step that can be further refined and improved. The goal is to remove the background of the plant

to identify only the features of the plant itself, independent of the environment or the background. This is achieved in the last component. The tray containing the plants must first be detected to achieve this goal. Subsequently, the plant within the tray must be cropped out and segmented into foreground and background. Based on this process, there are two primary components, as illustrated in Figure 5.2.

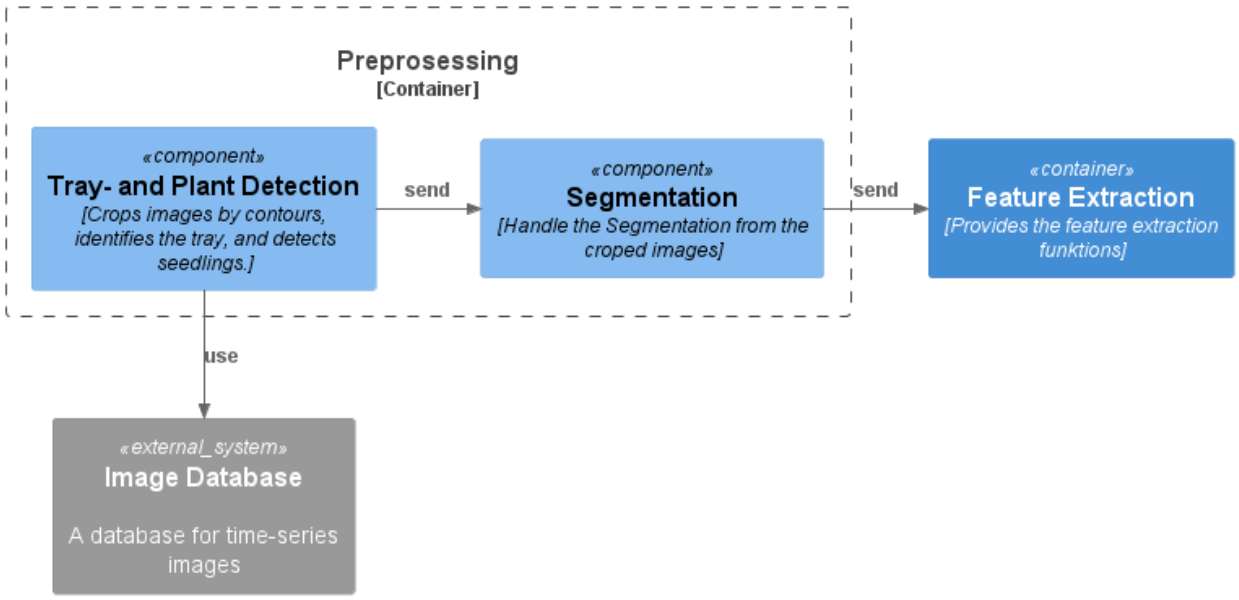

Figure 5.2: Component diagram showing the inner components of the Preprocessing container

5.2.1 Tray- and Plant Detection

This section describes the procedures and methods of the tray- and plant-detection components. The goal of this component is to obtain an image of one or more plants, which can then be segmented in the next component. This component marks the beginning of the entire pipeline.

For this thesis, a few species from the Eden ISS dataset will be selected. According to the objective of this thesis, which is to detect stress, a few of the plants from the selected species have to be stressed. Stress in the images was only found in the species *kohlrabi*, *tomato*, *cucumber*, and the *lettuce dragoon*. The stress assessment was undertaken by plant stress domain experts at the DLR Institute for Space Systems in Bremen, who worked in EDEN ISS during the fourth mission year of 2021/2022. The various images were sent to the

expert with the inquiry of which stress is introduced here, whereas the initial responses are contained in the appendix Table 8.2. A conclusion is made from the answer to understand the decision based on it.

- The stress in *lettuce dragoon*, caused by calcium tip burn and yellowing of older leaves, can be managed by choosing less susceptible cultivars and monitoring the plant's growth rate. Addressing these stresses through careful cultivar selection and growth rate management will significantly reduce their occurrence.
- For *kohlrabi*, the magnesium deficiency and potential other nutrient stresses can be managed by ensuring a well-balanced nutrient solution with sufficient magnesium.
- *Cucumbers* showing potassium deficiency and additional nutrient concerns can be managed by adjusting the nutrient solution to include adequate potassium levels. Removing brown lower leaves and monitoring past stress events will contribute to healthier plant development. Maintaining a well-balanced nutrient supply and good plant hygiene are key to preventing and managing these stresses.
- The dried debris, consisting of old leaves and stems, needs to be removed, which is normal for *tomato* plants. Additionally, a few leaves show symptoms of nutrient stress, although it is difficult to determine the specific nutrient(s) involved.

Given that the browning of leaves is a normal response for tomato plants and thus renders color-based detection ineffective, this thesis will focus on the species *lettuce dragoon*, *kohlrabi*, and *cucumber*. These plants were also selected because they represent common issues in greenhouse environments, including overlapping growth, species-specific plant detection, and high-growing varieties. Two distinct procedures have been developed to address these challenges for the three selected species, as described in the following section.

1. Case: Tray detection is performed by identifying contours based on the free area in the middle of the tray. After detecting the tray, individual cropping of each plant is carried out. Markers are placed in the middle of the tray, and the SAM (Segment Anything Model) is used to find the mask of the tray. Using this mask, plants are identified with a green threshold. The contours of each plant are then captured, and based on this information, the *lettuce dragoon* plants are cropped out.
2. Case: For *kohlrabi*, a different approach is required due to the significant overlap in the later growth stages. In this case, the image is split between the trays. Similar to

the kohlrabi image, the images from the cucumber will also be separated along an x coordinate. *Cucumbers* are usually placed in a rack with two trays, each containing one cucumber plant. This coordinate is selected manually and recorded in a configuration file for each time series of this type.

All methods result in images that can then be segmented with the methods explained in the next Subsection 5.2.2.

5.2.2 Segmentation

The plant segmentation is also a critical step in the preprocessing component, affecting all subsequent analyses and outcomes. As explained in the background in Section 3.2, some stress causes will first be visible on the edges of the leaves of a plant. Therefore, it is important to achieve high accuracy in the segmenting of plants. If the accuracy is low, it may lead to delayed detection of stress.

The methods for segmentation are selected based on several key criteria. Primarily, the selection is driven by EDEN ISS data. Since not all plants, such as red lettuce, use green as an indicator of health, the algorithm's underlying basis, mainly whether it relies on spectral data, is also considered. Additionally, the methods adhere to the principle of KISS (Keep It Simple, Stupid) [AB16], favoring simplicity whenever possible.
In this context, it is preferable that the algorithms do not require markers to specify which objects will be segmented. Otherwise, it would be necessary to develop a reliable method for the automatic identification of these markers. However, various methods, including those utilizing markers, will be employed to determine the most effective. Despite the effort required for their creation, the use of markers is justified by their potential benefits. Finally, the algorithms should be open-source and well-known.
The result of each method should be a binary mask that effectively masks the background of the plant. The goal of this comparison is to identify which of these algorithms provides the highest accuracy across a range of plant images, aiming to achieve a binary plant mask that accurately captures the edges and movements of the leaves.

First, a basic approach will be used due to its intuitive properties, ease of implementation, computational speed, and popularity in image segmentation. The threshold method will be the simplest method in this comparison [Go08], [AA19]. Since thresholds often prove difficult

and inaccurate in practice, requiring individual adjustments for each dataset, it is typically used with other preprocessing methods to achieve satisfactory results [Kr16]. For this test, a specific green threshold is determined for the plant phenotyping dataset, and additional methods such as erosion and dilation are employed to enhance accuracy when necessary. The threshold is found by fine-tuning the upper and lower threshold parameters and is measured against the ground truth mask from that dataset. In addition, this method is color-based, so changes in color due to a different data set, species variation, or environmental conditions may affect the results.

Furthermore, KMeans clustering has been selected for this implementation due to its simplicity and widespread popularity [CA79]. As one of the most fundamental and commonly used clustering algorithms, KMeans offers an intuitive approach that partitions data into distinct groups based on their features [DMC15], [GDD22]. Its ease of use and computational efficiency make it a preferred choice in many research studies and practical applications [Ce90]. Moreover, KMeans serves as a benchmark algorithm in numerous academic papers, providing a standard for comparison against more complex or specialized clustering methods [Mi22]. Its ability to produce clear, interpretable results allows researchers to effectively evaluate the performance of alternative techniques. Consequently, incorporating KMeans in comparative studies ensures a robust and comprehensive analysis of segmentation methodologies.

Another method is the SLIC (Simple Linear Iterative Clustering) algorithm, which is based on superpixels. Superpixels group pixels into perceptually meaningful atomic regions, thereby simplifying the image while preserving boundary information [SD23]. This approach leverages color-based segmentation and operates without the need for markers, making it an efficient and effective method for image analysis. The SLIC algorithm's ability to maintain essential image details while reducing complexity makes it a valuable tool in various applications, from object recognition to medical imaging [GDD22]. Its popularity stems from its balance of simplicity, accuracy, and computational efficiency [Sc16]. This method will be combined with the KMeans to result in the end in a binary mask like the other methods.

As an alternative that is not color-based, the Watershed algorithm is used as a comparison method. The Watershed algorithm interprets the grayscale image as a topographic surface, segmenting regions based on topographical features [Me94]. This method relies on the gradient of intensity values rather than color values, enabling effective segmentation in varied contexts. Additionally, the Watershed algorithm can be enhanced with markers to improve

segmentation results, allowing for more controlled and precise segmentation [HL09]. Its ability to use intensity gradients makes it particularly useful in these applications where color information is less relevant.

Finally, a deep learning variant, the SAM, is employed. SAM is a versatile model that leverages large amounts of training data to perform segmentation. It can segment objects in an image based on user-provided markers, points, or regions of interest [Ki23]. This model requires markers to select the desired mask but offers high accuracy and flexibility due to its advanced neural network architecture. The use of SAM demonstrates the potential of deep learning techniques in achieving superior segmentation performance, making it a valuable tool for a wide range of image analysis tasks [Sc16], [WMB23].

Table 5.1: Comparison of Image Segmentation Techniques

Segmentation Technique	Method	Markers Needed	Color-Based
Green Threshold	Thresholding	No	Yes
KMeans	Clustering	No	Yes
SLIC	Superpixel/Clustering	No	Yes
Watershed	Region Growing	yes	No
SAM	Neural Network	yes	No

To summarize the methods and the basis of the comparisons, the Table 5.1 summarizes all of them for a better overview. These methods are free to implement, and while most of the methods are available in the **skimage** library, the SAM algorithm is sourced from the Meta website. The KMeans clustering method has also been implemented using the **sklearn** library. Optuna, a library special for this kind of task, has been used to ensure that the different parameters are optimal for detecting the mask. [Ak19]
To compare the methods, Table 6.1 summarizes the results and shows which algorithm provides the highest accuracy over a range of plant images. The Plant Phenotyping dataset is used to evaluate accuracy. This dataset contains ground truth masks and is fundamentally similar to the EDEN ISS dataset, ensuring that the best method can subsequently be applied to the EDEN ISS dataset as well. In addition to accuracy, the speed of the algorithms is also evaluated and will be compared. For comparing accuracy, the Jaccard Index [GDD22], as well as True Positive (TP), True Negative (TN), False Negative (FN), and False Positive (FP) pixels are collected. These metrics are summarized in a binary confusion matrix.
The **Jaccard Index** (JI) is calculated as follows.

$$\text{JI} = \frac{|A \cap B|}{|A \cup B|}$$

It is a measure of how similar two sets are. It is calculated by dividing the size of the intersection of two sets by the size of their union. A represents the set of pixels labeled with the target class by the ground truth mask, and B represents the set of pixels labeled with the target class by the segmentation algorithm. The Jaccard similarity index measures the similarity and diversity of sample sets. The larger the value, the more similar the two objects are [GDD22].

Using the Jaccard Index provides a more comprehensive and robust analysis of the similarity between two sets. Ultimately, based on these evaluations, a decision will be made to identify the best segmentation method. The selected method will then be tested on the EDEN ISS dataset to validate its performance. The chosen method will be implemented in the segmentation component following this validation.

5.3 Feature Engineering

This section discusses the methods for the second research question and the identification of the best features. First, the metrics and methods used to extract features from the plant images will be explained. Additionally, the basic idea and concept behind the approach will be discussed. In addition to methods for visualization, statistical analysis, correlation methods, and redundancies between the different features are discussed. In addition to data analysis, methods for data preparation are explained. It is crucial to be able to work with and compare the data. The feature engineering component is divided into two components, Feature Extraction and Data Analysis, as shown in Figure 5.3.

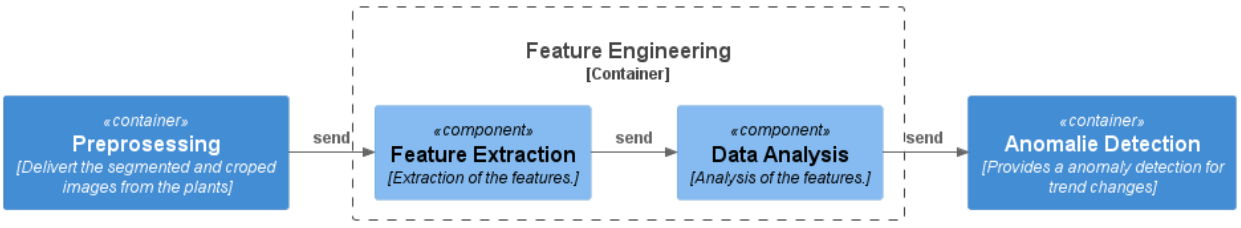

Figure 5.3: Component diagram showing the inner components of the Feature Engineering container

5.3.1 Feature Extraction

A key focus is identifying a principal feature based on spectral data, utilizing widely recognized indices such as GLI, VARI, and NDVI. These features are based on calculating spectral information, and the distinction between healthy and stressed plants has been extensively researched and proven [Gi21]. Spectral feature has deficits. For example, yellow leaves from lettuce are, in most cases, an indicator of plant stress. In other species, like cucumbers, the flower is yellow, so in this case, the feature would warn of stress. Another disadvantage is when a leaf has a red or another green colored leaf; then these indices cannot be compared directly to each other.

Other features are based on time and structure, examining the movement of a plant. Due to the temporal dimension of the dataset and based on the paper from [Ge21], where the movement of leaf angles is recorded and can be used to infer abiotic stress. In addition, [BG21] describes that stress depends on characteristics such as these explained in the Section 3.2 and on observations over time. Based on this, it was selected as a feature and evaluated in the course of the thesis. The advantage of these features compared to spectral features would be early detection, as the movement would develop in the first phases of plant resistance. In the following sections, the specific features and methods used to extract these features from the images will be explained in detail.

- **yellow_pixel_count**: First, the yellow_pixel_count feature is explored. A threshold method is employed to isolate the yellow and brown pixels in the images to extract this feature. The lower limit for this threshold is set to [20, 50, 75], where 20 represents the lower bound for the Hue channel, 50 represents the lower bound for the Saturation channel, and 75 represents the lower bound for the Value (brightness) channel. The upper limit is set to [35, 255, 255], with 35 as the upper bound for the Hue channel and 255 as the upper bound for both the Saturation and Value channels. This approach ensures that the relevant color information is accurately captured, focusing on the yellow and brown pixels within the specified ranges.
- **optical_flow_mag & optical_flow_ang**: To detect movement, the calcOpticalFlowFarneback method from OpenCV is employed to analyze changes between consecutive images. This technique calculates the motion of objects by comparing pixel intensities in sequential frames, providing information on dynamic changes. The results are represented by optical flow magnitude (optical_flow_mag), which measures the speed of motion, and optical flow angle (optical_flow_ang), which indicates the

direction of movement. Together, these components offer a detailed understanding of the movement within the image sequence.

- **edges**: Another feature of image analysis is edge detection, which helps to understand the boundaries within the images. The Canny method from OpenCV is employed with thresholds set at 100 and 200. This technique detects edges by identifying areas of rapid intensity change, providing crucial information about the structural details of the images.

- **SSIM**: Another feature for image analysis is the Structural Similarity Index (SSIM), measured using the structural_similarity function from the skimage.metrics module. This index is widely used in the field, effectively revealing structural changes within images. By examining these differences over time, SSIM proves to be a reliable indicator of structural variations [GDD22].

- **GLI & VARI**: Finally, popular indices such as the GLI and the VARI are added to the list of features. These indices are known for their effectiveness in various image analysis applications. The GLI emphasizes the presence of green vegetation by enhancing the green channel and reducing the influence of red and blue channels. The VARI is designed to be less sensitive to atmospheric effects, making it helpful in analyzing vegetation in varying atmospheric conditions. These indices' detailed calculations and further explanations are provided in Subsection 3.2.2. By including GLI and VARI as features, the analysis leverages its strengths in detecting and analyzing vegetation and other elements within images, enhancing the overall effectiveness of the image analysis process.

These features are collected over time to provide a comprehensive dataset for further analysis and decision-making in the next component.

5.3.2 Data Analysis

This section explains the data resulting from the methods used so far. Methods used to highlight the structure of the data and the importance of different feature time series are explained. The data understanding phase involves a detailed exploration and preparation of the dataset using statistical analysis, data visualization, and feature engineering techniques. This includes rolling statistics for time series data, correlation analysis, and Principal Component Analysis (PCA) for dimensionality reduction. These methods provide comprehensive

insight and robust preparation for effective predictive modeling.

The data understanding phase involves an examination of the data, utilizing a combination of statistical analysis and data visualization methods [Mo09]. These methodologies are crucial for gaining comprehensive insights into the structure and characteristics of the dataset, identifying anomalies or patterns, and laying the groundwork for subsequent analytical processes [JPW17].
This phase initially encompasses the creation of normalization and rolling statistics. Rolling statistics involve calculating summary statistics such as mean or standard deviation over a moving window of time steps. This technique is essential for capturing trends and smoothing out short-term fluctuations, thereby providing a clearer view of the underlying patterns in the time series data.
In addition to these time series-specific methods, a correlation analysis will explore the relationship between variables. This involves calculating correlation coefficients, which measure the strength and direction of linear relationships between pairs of variables. A high correlation between variables can indicate redundancy, while a low correlation can highlight potentially important independent variables. Understanding these relationships is critical for effective feature selection and model building.
Following the correlation analysis, PCA is performed. PCA is a dimensionality reduction technique that transforms the data into a new set of variables called principal components [HG15]. These components are linear combinations of the original variables and are ordered such that the first few retain most of the variation in the original dataset. By reducing the dimensionality, PCA helps highlight the most essential features, mitigating multicollinearity and reducing computational complexity, which is particularly beneficial when dealing with high-dimensional data.
By systematically applying these methods, the data understanding phase aims to create a solid foundation for building effective and reliable predictive models. These techniques collectively ensure that the data is well-prepared and relevant features are selected, leading to more accurate and generalizable outcomes.

5.4 Anomaly Detection

This section explains the methods to find when the first stress was detected. this part can be divided into two tasks. First, the classification of stressed and healthy plants includes finding the time point when the trend has differences to the healthy pattern. and second,

finding the accuracy of the detected change points, when stress has an impact on the plant. While a labeling in healthy and stress plants is there, no labeling for the individual plants and the point, when a human can see the stress is available. The concept of the Anomalies Detection container is shown in the Figure 5.4, and the methods will be explained in the following.

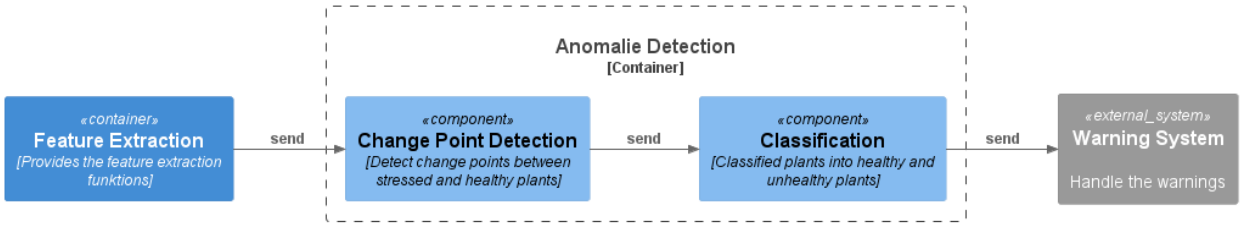

Figure 5.4: Component diagram showing the inner components of the Anomaly Detection

A data-driven approach based on the data and the expected results will be used to find the best method for detecting the time of the first stress responses in plants. This means that a supervised approach will be unsuitable because there are only a few healthy and stressed labeled data. An unsupervised approach cannot distinguish between the healthy and stressed data based on their structure, as the knowledge of what constitutes a healthy plant time series cannot be collected or trained. In the end, semi-supervised learning approaches are the selected methods.

In this work, novelty detection with the LOF is used to identify change points in the time-series data of plants. For each aligned time series, feature vectors are created using a sliding window. These vectors serve as input for the LOF model. The LOF model is trained on the feature vectors of the healthy training data and then applied to the test data to detect anomalies. Anomalies that show significant deviations from neighboring data points are identified as potential stress points [Al21]. The first detected anomaly in each time series is considered a change point. The LOF method was chosen because it effectively highlights differences by evaluating density deviations of neighboring data points [Te10]. This approach is particularly useful for detecting local outliers that might be overlooked in global analyses [BBS22]. Additionally, novelty detection allows for identifying new patterns that may indicate significant changes or unknown events [Ya20], [SS19]. Optuna is used to find the best model parameters and maximize anomaly detection accuracy. Overall, LOF enables effective detection of stress points in plants, providing important insights into their health and condition.

The selection of this method allows for an effective analysis of the specific characteristics of the time series, considering their unique properties. The application of the LOF method,

supported by PCA analysis, has proven advantageous as it makes significant deviations in the data visible.

To evaluate this method, the model will first be trained using data from the species dragoon lettuce, cucumber, and kohlrabi. These datasets, which have been visually labeled, will be used for comparison through a confusion matrix. This comparison focuses solely on the classification of the plants. The plants will be classified as stressed if a change point or anomaly is detected. For a comparable analysis, an equal number of healthy and stressed plants will be used for each species, ensuring that the length of the smaller dataset, after division into test and training sets, matches the length of the other datasets.

The method will be evaluated using labeled plant data to determine the effectiveness of classifying stressed plants. The confusion matrix will facilitate this comparison, highlighting the classification performance of the LOF method. Subsequently, the accuracy of the LOF method in detecting change points will be visually compared across different plant species from the EDEN ISS data. This comprehensive analysis will provide insights into the effectiveness of the method for identifying plant stress and assessing its applicability to various plant species.

6 Experiments

This chapter provides an overview of the results of the different methods used, which were described in the previous chapter. It starts with a comparison of different segmentation algorithms and the selection of the best algorithm for the EDEN ISS data, the results of the different species and their methods from the component preprocessing are also presented. Subsequently, the results and the subsequent methods of the Feature Engineering component are further processed. The results are presented again, and the results or best features are used in the following component. In the last component, these results are used and presented for an evaluation of a change point detection method. This includes a comparison of the classification of the different species and also a visual comparison of the accuracy of the detected change points algorithms.

6.1 Segmentation Comparison

Initially, this section presents the results of comparing various segmentation methods for background removal from plant images. The first focus should be on the Plant phenotype dataset to evaluate the performance of these methods based on the ground truth mask in this dataset. The methods were chosen in Section 5.2 based on their different approaches, deliberately excluding deep learning algorithms that require training. In addition to the results on the Plant Phenotype dataset, we also examine the results on the EDEN ISS dataset. Although these datasets appear similar at first glance, they differ in specific challenges, allowing for a comprehensive evaluation of the segmentation methods. The methods on the EDEN ISS dataset are evaluated visually due to the lack of ground truth masks. Finally, the most suitable method on the EDEN ISS dataset will be selected for further work. For the tests performed in the following sections, the optimal parameters for each method were first determined using Optuna on a single image with a corresponding ground truth mask. These parameters were then kept constant throughout the subsequent evaluations. However, after a first comparison of the EDEN ISS dataset, the parameters were adapted to the specific species of this dataset.

6.1.1 Plant Phenotyping Dataset Segmentation

In Figure 4.5, five images represent different samples of the same plant species from the Plant Phenotype dataset. These images are supported by segmentation masks, facilitating a comprehensive evaluation of various segmentation methods. As explained in the Section 5.2, the study focused on five segmentation methods: Green Threshold, SLIC+KMeans, SAM, KMeans, and Watershed. Each method was assessed for its effectiveness in accurately segmenting the plant images, with a metric such as the Jaccard Index being calculated. Additionally, the computational efficiency of each method was measured in terms of average processing time.

Figure 6.1: Results of different segmentation methods for a single plant

The average results of all 18 plants, which have 16 images long-time series, are summarized in Table 6.1. This revealed that the SAM method averaged the highest performance across the Jaccard and Dice indexes, demonstrating superior precision while achieving a computation time of 68.88s, a significant difference from the other method and a highly time-consuming efficiency. This method also needs a marker for accurate detection, which requires another detection method for this part, then again. With only one point behind the SAM method, the Green Threshold method has the shortest computing time of all methods. The third accurate method is the Watershed method, which has nearly the same accuracy and computing time. The last methods have about the same accuracy; only the computing time is double that of the SLIC+KMeans method. There is a 0.45 Jaccard index for the SLIC+KMeans and 0.46 for the KMeans alone.
To better understand the results from the KMeans and the SLIC+KMeans, the Figure 6.2 is shown. In this image, the bad results from both algorithms can be explained. Because the methods do not use markers or the color green as an indicator for plants. These methods

Table 6.1: Results of Segmentation Methods

Method	**Average Jaccard Index**	**Average Dice Coefficient**	**Accuracy**	**Average Time (seconds)**
Green Threshold	0.90	0.94	0.96	0.00
SLIC + KMeans	0.45	0.50	0.53	0.42
Segment Anything Model (SAM)	0.91	0.95	0.97	68.88
KMeans	0.46	0.50	0.53	0.28
Watershed	0.89	0.94	0.95	0.04

cannot identify which mask is foreground and background.

Green Threshold Jaccard: 0.80 | SLIC+KMeans Jaccard: 0.01 | SAM Jaccard: 0.81 | KMeans Jaccard: 0.01 | Watershed Jaccard: 0.73

Figure 6.2: Examples of incorrect mask predictions

The next part is meant to strengthen the previous statements and explain how the methods work. Based on the results, KMeans and SLIC+KMeans are excluded from further analysis of this dataset. The following diagrams show the progression of the Jaccard Index for the three remaining methods over time. The X-axis represents the different time points from the plant images shown here Figure 4.6 at which the Jaccard Index was measured, while the Y-axis shows the values of the Jaccard Index. The line represents the mean Jaccard Index, and the shaded area around the line represents the standard deviation, illustrating the variability or dispersion of the Jaccard Index values at each time point.
The Green Threshold method, shown in Figure 6.3 starts with a high Jaccard index and decreases over time. The shaded area around the mean line indicates increasing variability, indicating that the method is struggling to maintain consistent performance. This increasing variability reflects the sensitivity of the method to changing background conditions. The increasingly greener background significantly affects the accuracy of the measurements, resulting in a decrease in the Jaccard index.

The Watershed method in Figure 6.4 shows similar behavior to the Green Threshold method. It also starts with a high Jaccard index that decreases over time. The increasing variability, shown by the widening shaded area, indicates that the method becomes less consistent as the background becomes greener. This increasing variability suggests that the performance of the method is negatively affected by changes in the background, reducing the accuracy of

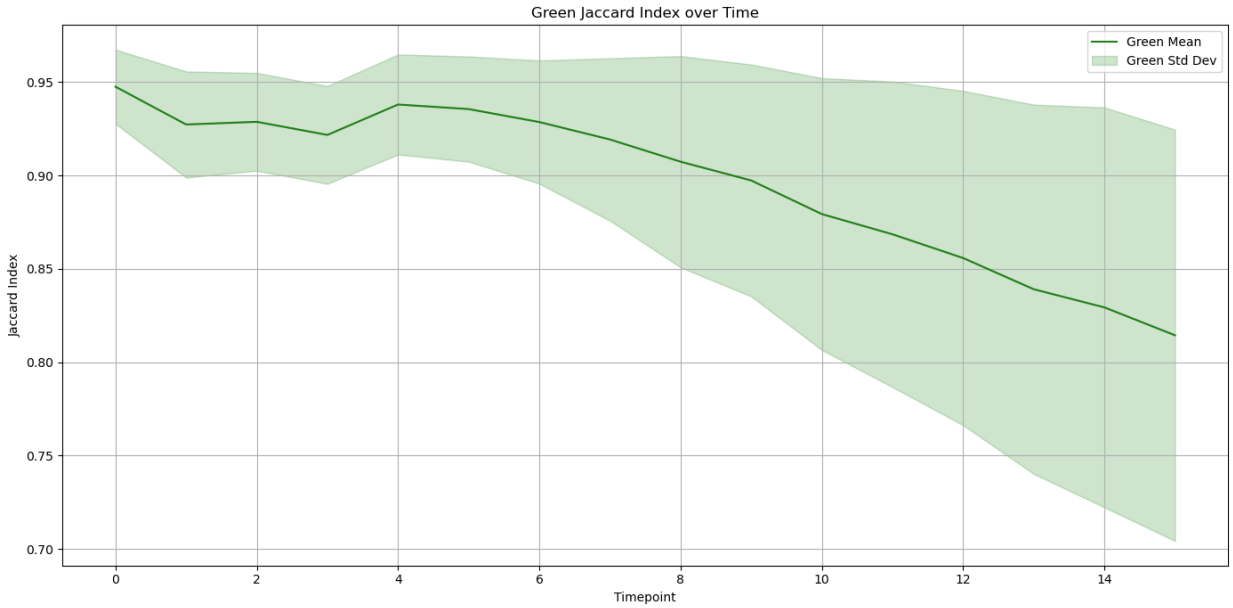

Figure 6.3: Jaccard index over time using the Green Threshold method

the measurements.

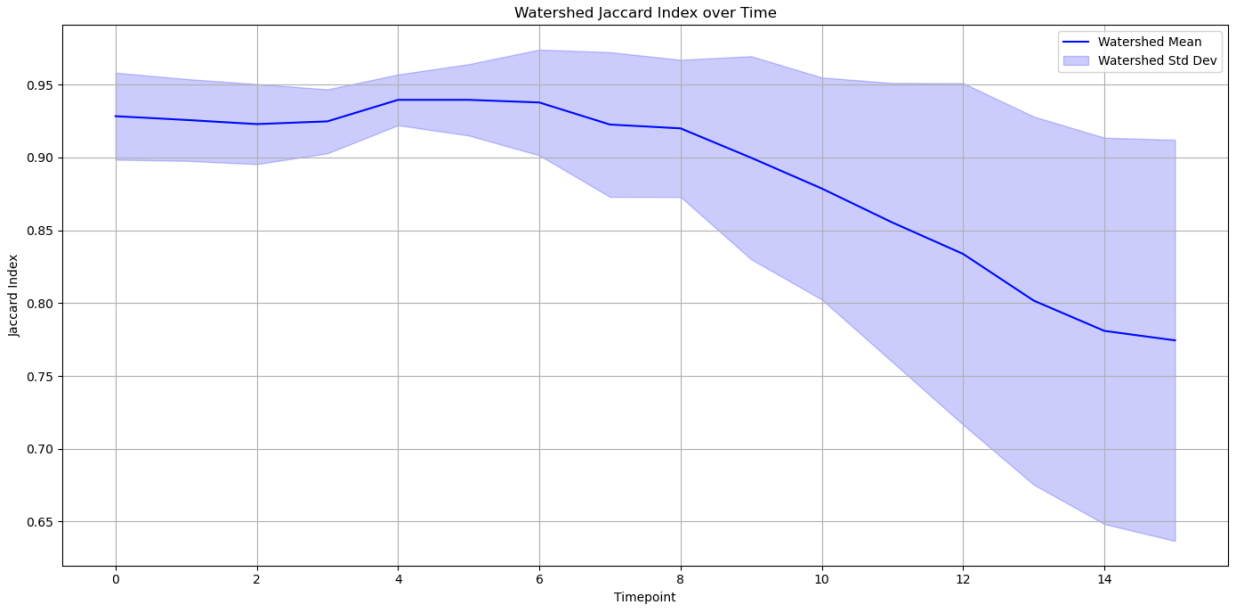

Figure 6.4: Jaccard index over time using the Watershed method

In contrast, the SAM method in Figure 6.5 shows a different behavior. It initially reaches a relatively high Jaccard index and shows significant fluctuations in the early stages, as

indicated by the wide shaded area around the mean line. This indicates a high variability in the Jaccard Index values. Over time, however, the Jaccard index for the SAM method stabilizes, and the variability decreases. Despite these initial fluctuations, the Jaccard index of the SAM method remains relatively constant on average over the observation period. This suggests that, after an initial adjustment period, the SAM method provides more stable results and is less influenced by changes in the background.

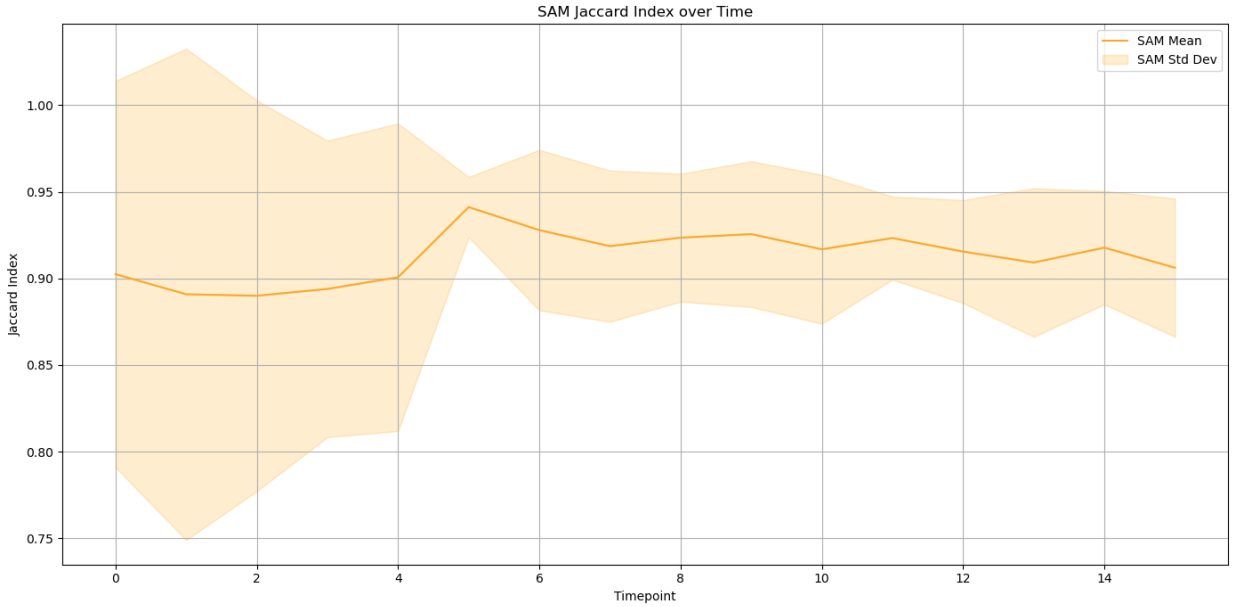

Figure 6.5: Jaccard index over time using the SAM method

The results indicate that the Green Threshold and Watershed methods are more sensitive to background changes, resulting in decreased accuracy and increased variability. In contrast, the SAM method shows better stability and consistency of performance, especially after the initial fluctuations. This makes it a more robust choice for segmentation in dynamic environments.

6.1.2 EDEN ISS Dataset Segmentation

A significant advantage is that the background of the Eden ISS images does not change much, except for some overlap. To validate the previous results on this dataset, all segmentation methods are now performed on one image for each selected species from the EDEN

ISS dataset.

For the markers from the phenotyping dataset, the ground truth mask was used. Therefore, markers must be created for the EDEN ISS data for this comparison. In the images, these markers are shown as red dots; they have been hard-coded and manually selected. All other data sets remain unchanged, and a visual comparison does the evaluation.

Figure 6.6: Segmentation results for a dragoon lettuce plant using different segmentation methods

As seen in the Figure 6.6, the different results from each method are shown. The first image is the original image, with the markers for the Sam as red points. The results show that the masks produced by the KMeans, SLIC+KMeans, and Watershed methods frequently misidentified the foreground, leading to inaccurate segmentations. In contrast, the SAM method proved to be the most accurate, producing a clear and accurate segmentation mask. The Green Threshold method also performed well and was ranked as the follow-up method, largely correctly separating the plant from the background.

Figure 6.7: Segmentation results for a kohlrabi plant using different segmentation methods

The Figure 6.7 illustrates the segmentation outcomes for kohlrabi. The initial image is the original, annotated with red points indicating the markers for the SAM method. It is evident from the results that the masks generated by the KMeans, SLIC+KMeans, and Watershed

methods frequently misclassified the foreground, resulting in imprecise segmentations. On the other hand, the SAM method showed superior accuracy, producing a precise and clear segmentation mask. Similarly, the Green Threshold method performed commendably, recognized as the second-best method due to its effectiveness in distinguishing the kohlrabi plant from the background.

Figure 6.8: Segmentation results for a cucumber plant using different segmentation methods

In the Figure 6.8, the segmentation results for cucumber are depicted. The first image is the original one, with red points indicating the SAM method's markers. The analysis reveals that the KMeans, SLIC+KMeans, and Watershed methods often failed to correctly identify the foreground, leading to erroneous segmentations. Conversely, the SAM method emerged as the most reliable, providing an accurate and well-defined segmentation mask. The Green Threshold method also exhibited strong performance, considered the runner-up method for effectively isolating the Cucumber plant from the background.
In summary, the SAM method demonstrated the highest accuracy in segmentation results across all three species: dragoon lettuce, kohlrabi, and cucumber. This method relied on specific markers manually selected and hard-coded to ensure precise segmentation. Conversely, while performing commendably, the Green Threshold method was not specifically optimized for this dataset; it was applied in its original form as used in the plant phenotyping dataset. The KMeans, SLIC+KMeans, and Watershed methods exhibited significant limitations in accurately identifying the foreground, resulting in less precise segmentations. Given these observations, a subsequent analysis will compare the performance of an optimized Green Threshold method against the SAM method to provide a more thorough evaluation.

The segmentation results for three different plant types using the SAM method and the optimized green threshold method are presented in the following Figures. Each figure includes the original image with marked points, the SAM method, and the optimized green threshold segmentation.

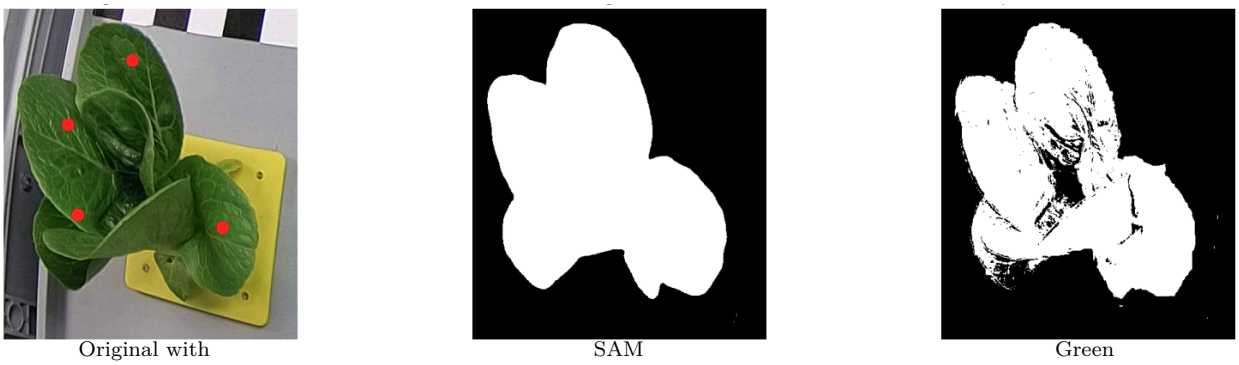

Original with Points | SAM | Green Threshold

Figure 6.9: Segmentation result for a dragoon lettuce plant using an optimized green threshold with the Green Threshold method in comparison to SAM segmentation

In Figure 6.9, the dragoon plant is segmented using both methods. The SAM segmentation effectively isolates the plant from the background, accurately capturing the overall shape. The optimized green threshold method also performs impressively, closely matching the SAM results by accurately delineating the plant's shape with minimal noise. The slight artifacts present are negligible, showcasing the green threshold method's effectiveness after optimization.

Original with Points | SAM | Green Threshold

Figure 6.10: Segmentation result for a kohlrabi plant using an optimized green threshold with the Green Threshold method in comparison to SAM segmentation

Both methods demonstrate strong performance for the kohlrabi plant in Figure 6.10. The SAM method provides a clean segmentation, accurately identifying the plant's leaves. After refinement, the optimized green threshold method shows significant improvement, closely approximating the SAM results. The background noise is substantially reduced, and the plant is clearly separated, proving the method's robustness in handling complex structures

and backgrounds.

Figure 6.11: Segmentation result for a cucumber plant using an optimized green threshold with the Green Threshold method in comparison to SAM segmentation

Figure 6.11 displays the segmentation results for the cucumber plant. The SAM method continues to perform well, producing a precise segmentation of the plant. The optimized green threshold method demonstrates notable enhancement, successfully capturing the plant's contours with minimal noise. The segmentation quality is nearly on par with the SAM method, highlighting its ability to handle varying green shades and complex backgrounds effectively. Overall, both the SAM segmentation method and the optimized green threshold method provide high-quality segmentations across all three plant types. While the SAM method consistently offers precise and clean results, the optimized green threshold method achieves nearly comparable accuracy with its recent improvements. This comparison underscores the effectiveness and reliability of both methods for plant segmentation tasks, with the optimized green threshold method emerging as a solid alternative to the SAM method. The green threshold method is the simplest and fastest algorithm, and it can be adjusted to suit each specific plant. This method efficiently utilizes plants' characteristic green color to separate them from the background, making it quick and easy to implement. On the other hand, the SAM method requires markers, necessitating using another method to accurately identify these markers. Additionally, SAM is relatively slow but highly precise in its segmentation results.

Despite the high accuracy of the SAM method, the Green Threshold method is used for practical applications because of its simplicity, speed, and adaptability to different plants.

6.2 EDEN ISS Results

This chapter presents all the Plant Stress Detection System (PSDS) outcomes. The pipeline initiates with preprocessing as elucidated in the Chapter 5. For the EDEN ISS dataset, this entails detecting the tray and cropping the images, in the case of the dragoon lettuce. Following preprocessing, segmentation is applied to the images. The outcomes of this segmentation will be discussed individually for each of the three species.

6.2.1 Preprocessing

The preprocessing results will first be presented, showcasing the outcomes for the dragoon lettuce. This is the first and most complicated case because the plant must be found and cut out based on the contour. In addition, for accurate and reliable detection, it is essential to detect the outline of the tray as well. Then, the results of the second case from the preprocessing are shown for kohlrabi and cucumber species.

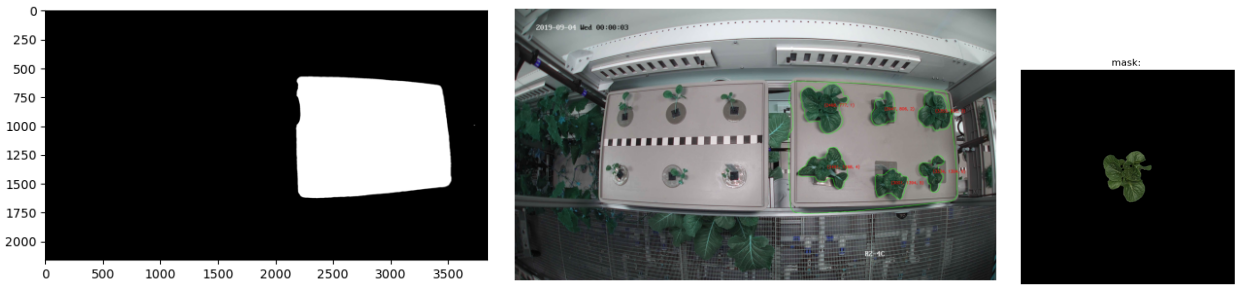

(a) mask of detected tray (b) detected plants inside of the tray mask (c) croped and segmented image

Figure 6.12: Overview of the preprocessing artifacts for a tray of dragon lettuce plants

The first Figure 6.12(a) shows the mask detected by identifying the central free area in the image and then cropping it using the SAM. This process is critical for isolating relevant areas for further analysis. The second Figure 6.12(b) shows the detection of the plants in the tray. This detection is based on the coordinates in the original image, allowing for precise identification of the plant positions. The plants are then cut out based on their contours, ensuring accurate separation from the background. After plant extraction, the image is processed in the segmentation component. The result of this segmentation is shown in the third Figure 6.12(c), which shows the final segmented image. This segmented image is a detailed representation of the structure and features of the plant, which is essential for subsequent analysis.

The detection of the trays using the free area detection and the SAM algorithm did not always give satisfactory results, which affected the whole pipeline. In addition, the initial detection of seedlings was also not always successful because, in the case of overlapping plants, the contours of two plants would merge, causing them to be cut out together. These errors also affect the subsequent pipeline and require manual data validation.
In contrast, plant segmentation is generally reliable and relatively accurate. Despite the challenges of tray and seedling detection, segmentation provides consistent and accurate results that are critical for further analysis of the plants.

Next, the second case for the kohlrabi and cucumber plants is addressed. In this case, the images are split vertically to divide the trays. The position for this division is hard-coded in the metadata in Section 4.1 of each time series. This vertical splitting of the images allows a clear distinction between the trays, ensuring that each tray can be analyzed individually.

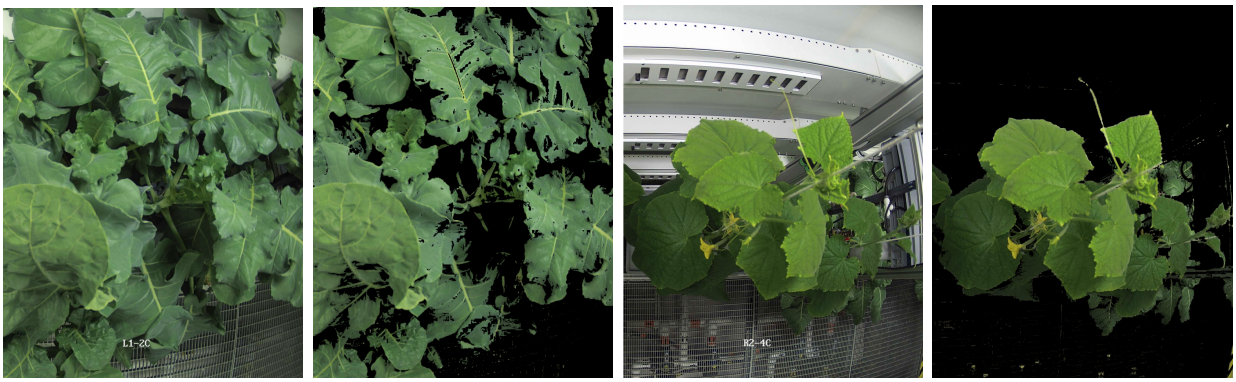

(a) croped kohlrabi (b) segmented kohlrabi (c) croped cucumber (d) segmented cucumber

Figure 6.13: Example images of a kohlrabi and a cucumber plant before and after segmentation

In Figure 6.13 (a) shows an initial image of a kohlrabi plant, demonstrating the state of the plant at the beginning of the pipeline after vertical division based on the x-coordinate. The kohlrabi and the cucumber images follow a similar processing path as outlined in case 1, culminating in the results shown in Figure 6.13 (b).
The results are also comparable because of the similarity of the methods applied to the kohlrabi and cucumber plants. Figure 6.13(c) shows the at the saved x-coordinate split line, kohlrabi example while Figure 6.13(d) shows an example of the segmented results for this cucumber plant, highlighting the consistency and precision of the segmentation process across different plant species. This demonstrates the robustness and applicability of the

methodology to different types of plants. The next chapter examines the results derived from the preprocessing steps, focusing on the features associated with the dragon lettuce in the initial case study.

6.2.2 Feature Engineering

In modern data analysis, precise processing features are crucial for obtaining reliable and meaningful results. This process comprises several key steps: extracting relevant features, their normalization, and their adjustment to a uniform length using a rolling-windows analysis.

Feature extraction is the first and fundamental step in data preparation. In this step, the features outlined in Chapter 5 are extracted from the dataset. Careful selection of features is essential to reduce the complexity of the data. The second step involves the normalization of the extracted features. Normalization is an essential process to eliminate differences in the scales and units of the features. By applying Min-Max scaling, the data are brought to a comparable range. This is particularly important to avoid distortions and ensure that each feature contributes equally to the analysis. Finally, the normalized features are standardized to a uniform length using a rolling-windows analysis. This method analyzes time-dependent data using sliding time windows in fixed intervals. The two graphs below illustrate the difference in the data before and after applying normalization and the rolling-windows analysis.

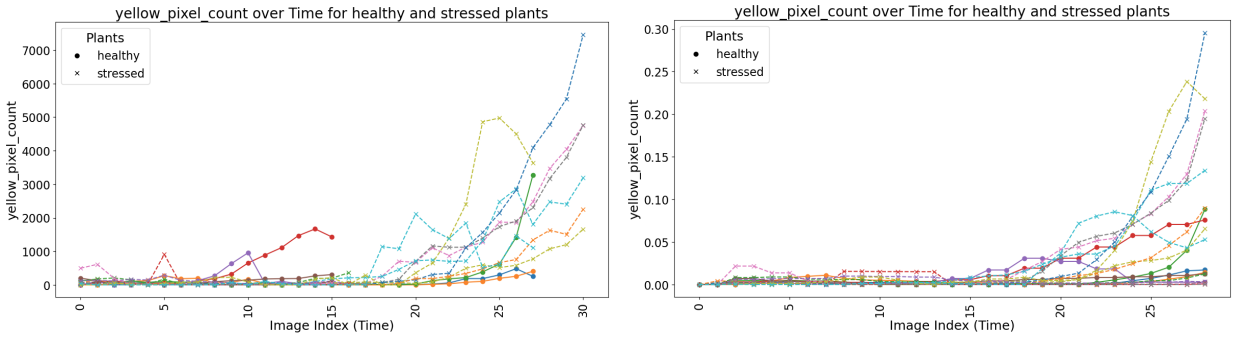

(a) orignal yellow_pixel_count

(b) normalized and uniform length yellow_pixel_count

Figure 6.14: Example of applying a rolling window to yellow_pixel_count in the dragon lettuce data

In the first Figure 6.14(a), it is evident that the yellow pixel counts vary significantly across different time intervals. These raw data show considerable differences in the length and scal-

ing of the time series. After applying the normalization and the rolling-windows analysis, the data are standardized to a uniform length as shown in the second Figure 6.14(b). This greatly facilitates comparison and further analysis, as all features have a consistent structure. Combining these three steps, extraction, normalization, and rolling-windows analysis, creates a robust and coherent data foundation, serving as the basis for further analyses and modeling.

To demonstrate the interrelationships among the various features from the three species, a correlation matrix has been constructed and is presented in Figure 6.15. This matrix provides a comprehensive overview of the pairwise correlations between the features, thereby highlighting potential dependencies and associations that may inform further analysis.
These features include the number of yellow_pixel_count, the SSIM, the number of edges, the optical_flow_ang, the GLI, the optical_flow_mag, and the VARI. Correlations range from -1, indicating a perfect negative correlation, to 1, indicating a perfect positive correlation, while a correlation of 0 means, there is no correlation. The analysis of the correlation matrix reveals a strong negative correlation of -0.76 between SSIM and optical_flow_mag. This significant correlation implies that an increase in one feature leads to a substantial decrease in the other, highlighting the presence of high redundancy. Similarly, a strong negative correlation of -0.55 between SSIM and GLI further underscores the redundancy issue. The features edges, GLI, and optical_flow_mag also show moderate positive correlations with each other, with values between 0.49 and 0.75, indicating that they contain similar information and could, therefore, be redundant. In contrast, the yellow_pixel_count feature shows generally low correlations with the other features, with values between -0.16 and 0.25. This suggests that yellow_pixel_count is mainly independent of the other features. Similarly, the optical_flow_ang feature shows generally low to moderate correlations with the other features, justifying its retention. Based on these observations, the following features are excluded: SSIM is excluded because it shows strong negative correlations with several other features, indicating high redundancy. Edges and GLI are excluded because they show moderate positive correlations with several other features, making them redundant. This decision was made to streamline the analysis and avoid multicollinearity. The features yellow_pixel_count and optical_flow_ang, with their low correlations with the other features, stand out as potential sources of valuable, independent information for the analysis. Removing these redundant features reduces model complexity, improves interpretability, and potentially optimizes model performance. The remaining features should provide sufficient information for accurate modeling, leading to a more efficient and robust model structure.

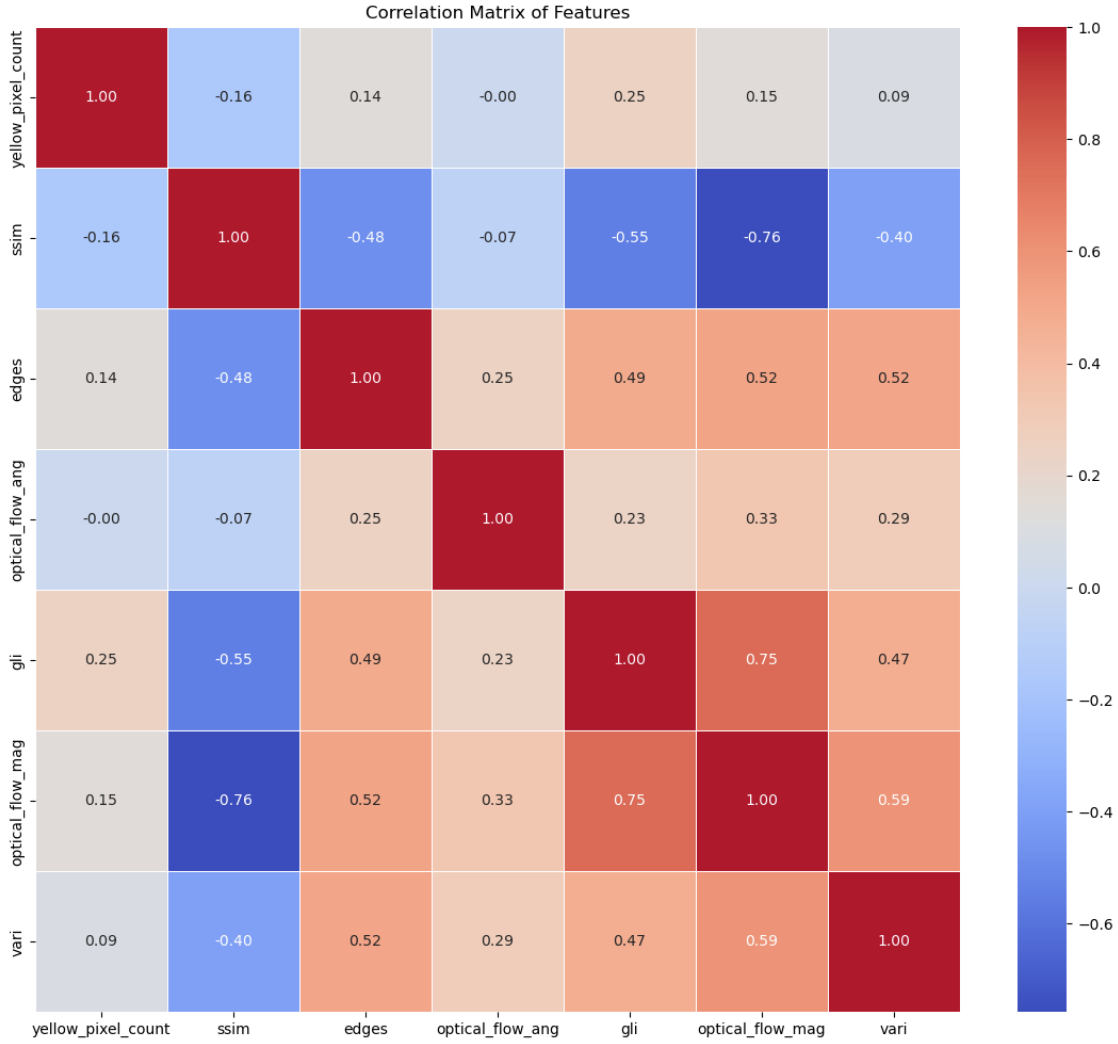

Figure 6.15: Correlation matrix over the dragoon lettuce, kohlrabi, and cucumber datasets and all selected features

The Figure 6.16 is a scatter plot displaying the results of the PCA. The data points are color coded, with red representing "Unhealthy" and green representing "Healthy". The x-axis represents the first principal component, while the y-axis represents the second principal component. The chart clearly separates healthy and unhealthy samples along the principal components. The majority of the healthy data points (green) are clustered near the origin (0,0) of the principal component axes, indicating less variance among the healthy samples. In contrast, the unhealthy data points (red) are more dispersed, indicating more significant variability. This separation shows that the PCA effectively differentiates healthy from unhealthy samples for the dragoon lettuce based on the given features.

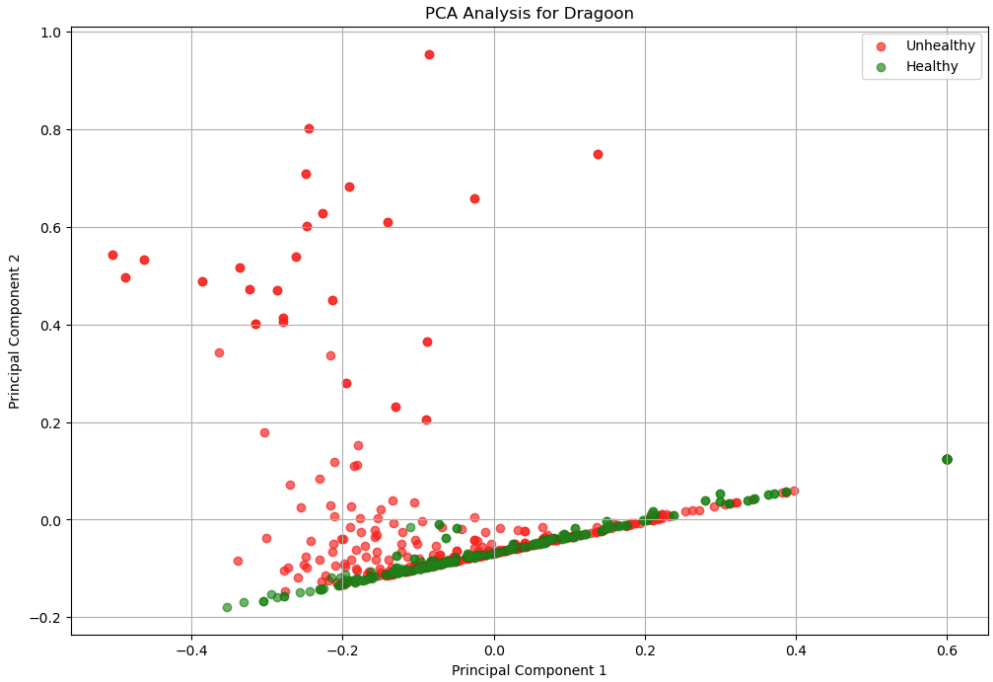

Figure 6.16: Results of the PCA analysis for the dragon lettuce dataset

The Figure 6.17 is a bar graph illustrating the contributions of two features—yellow_pixel_count and optical_flow_ang to the first two principal components. For the first principal component (blue), yellow_pixel_count shows a significantly negative contribution, while optical_flow_ang also has a negative contribution. For the second principal component (orange), yellow_pixel_count has a positive contribution, while optical_flow_ang also has a positive but minor contribution. Both features contribute differently to each principal component. These differentiated contributions help understand how each feature influences the variance in the PCA transformation. The negative and positive contributions illustrate the direction in which the features influence the principal components. For example, a negative contribution of yellow_pixel_count to the first principal component suggests that higher values of this feature correlate with lower values along the first principal component.
From the second Figure 6.17, it becomes evident that yellow_pixel_count plays a pivotal role in distinguishing the data in the PCA, compared to optical_flow_ang. This is due to yellow_pixel_count making significant contributions to both the first and second principal components, while the contributions of optical_flow_ang are relatively smaller. Therefore, yellow_pixel_count is a more influential feature in explaining the variance in the data and supporting the classification of samples (healthy vs. unhealthy) for the dragoon lettuce data.

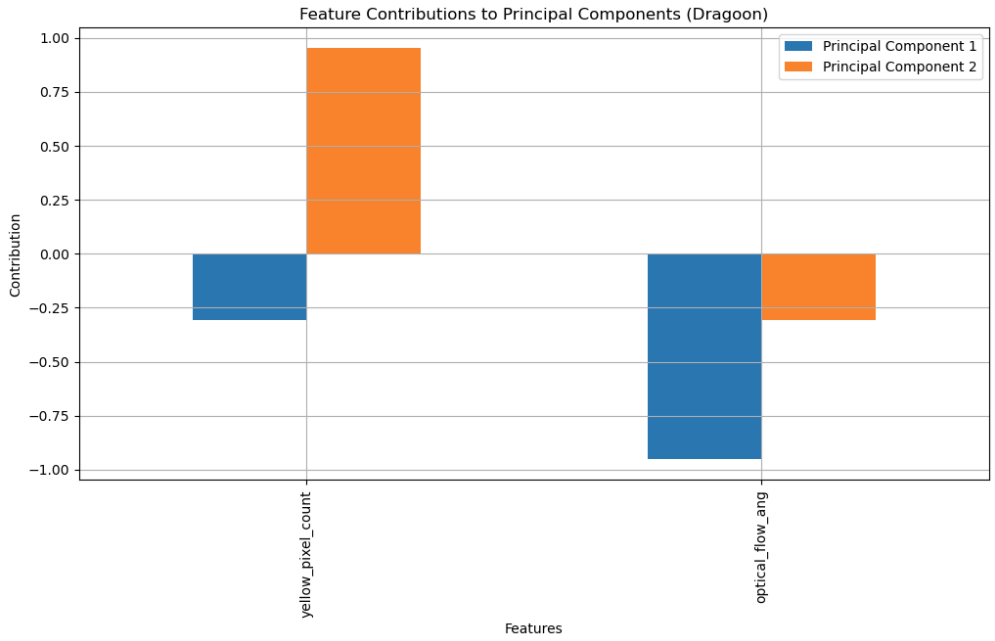

Figure 6.17: Feature contribution to PCA from dragon lettuce dataset

Combining these two charts offers a comprehensive perspective on analyzing the dragoon lettuce data using PCA. The scatter plot demonstrates the effectiveness of PCA in separating healthy and unhealthy samples, while the bar graph highlights the importance of each feature in defining the principal components. This analysis is valuable for further diagnostic or predictive modeling tasks related to the dragoon lettuce data.

Based on the dragoon lettuce data analysis, a detailed cucumber data analysis using PCA is presented as follows. The Figure 6.18 shows the provided scatter plot, and the results of the PCA are displayed. As before, red data points represent "Unhealthy," and green data points represent "Healthy." The axes represent the first and second principal components. The plot clearly separates healthy and unhealthy samples along the principal components. Most healthy data points (green) are clustered closer to the origin (0,0) of the principal component axes, indicating lower variance among the healthy samples. In contrast, the unhealthy data points (red) are more widely dispersed, indicating more significant variability. This separation demonstrates that the PCA effectively differentiates healthy from unhealthy cucumber data based on the given features.
The Figure 6.19 is the corresponding bar chart illustrating the contributions of the two features to the first two principal components. For the first principal component (blue), yellow_pixel_count shows a small negative contribution, while optical_flow_ang exhibits

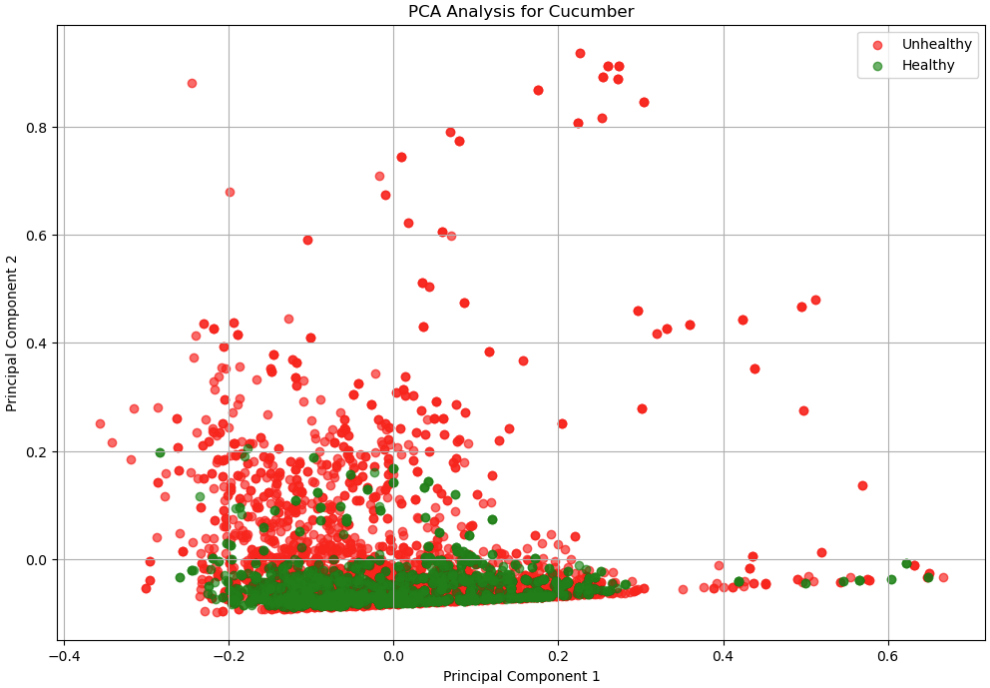

Figure 6.18: Results of the PCA analysis for the cucumber dataset

a significant negative contribution. For the second principal component (orange), yellow_pixel_count has a solid positive contribution, while optical_flow_ang shows a small positive contribution.

Regarding the relevance of each feature's contribution to the separation of the data in the two principal components, yellow_pixel_count has a minor negative contribution to PC1 but a significant positive contribution to PC2, indicating its importance in PC2. optical_flow_ang shows a significant negative contribution to PC1 and a small positive contribution to PC2, suggesting it is more influential in PC1 but also relevant in PC2.

There are no significant differences between the outcomes of the cucumber and dragoon lettuce data. Based on the contributions to the principal components, it can be concluded that both yellow_pixel_count and optical_flow_ang are useful features for separating the data in the PCA on the cucumber data, with yellow_pixel_count being more relevant for PC2 and optical_flow_ang being more relevant for PC1.

The final PCA was also performed on the kohlrabi part of the data, which is presented below. In the scatter plot, the results of the PCA for the kohlrabi data are displayed. As before, the red data points represent "Unhealthy" samples, while green data points represent "Healthy" samples, and the axes represent the first and second principal components. The plot clearly separates healthy and unhealthy samples along the principal components. Most healthy

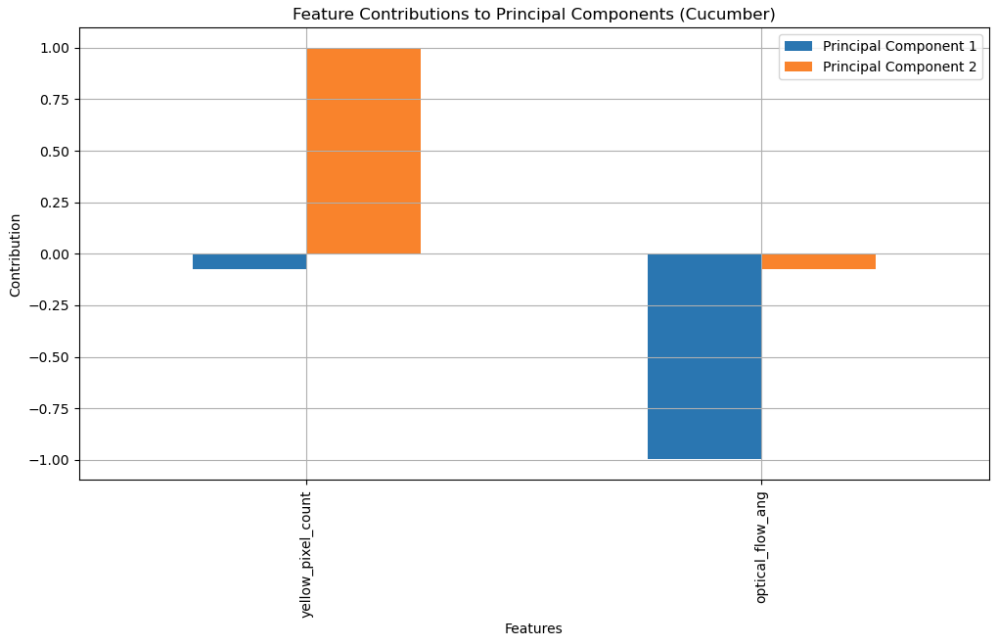

Figure 6.19: Feature Contribution to PCA from Cucumber Dataset

data points (green) are clustered closer to the origin (0,0) of the principal component axes, indicating lower variance among the healthy samples. In contrast, the unhealthy data points (red) are more widely dispersed, indicating more significant variability. This separation demonstrates that the PCA effectively differentiates healthy from unhealthy samples based on the given features.

The corresponding bar chart shows the contributions of two features to the first two principal components. For the first principal component (blue), yellow_pixel_count shows a significant positive contribution, while optical_flow_ang exhibits a substantial negative contribution. For the second principal component (orange), yellow_pixel_count has a notable negative contribution, while optical_flow_ang shows a considerable positive contribution.

Regarding the relevance of each feature for separating the data in the two principal components, yellow_pixel_count has a significant positive contribution to PC1 and a notable negative contribution to PC2, indicating its importance in both components but more influential in PC1. optical_flow_ang shows a substantial negative contribution to PC1 and a considerable positive contribution to PC2, suggesting it is more influential in PC2 but also relevant in PC1.

The results of the kohlrabi data are consistent with previous analyses and do not show significant differences. Both yellow_pixel_count and optical_flow_ang are essential features for separating the data in the PCA, with yellow_pixel_count being more relevant for PC1

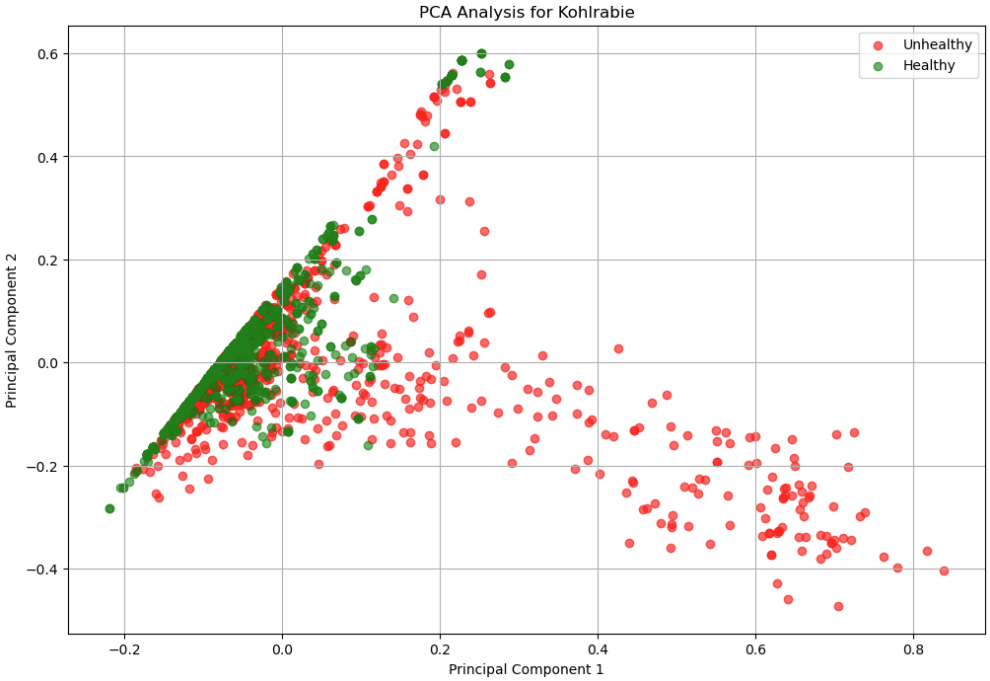

Figure 6.20: Results of the PCA analysis for the kohlrabi data

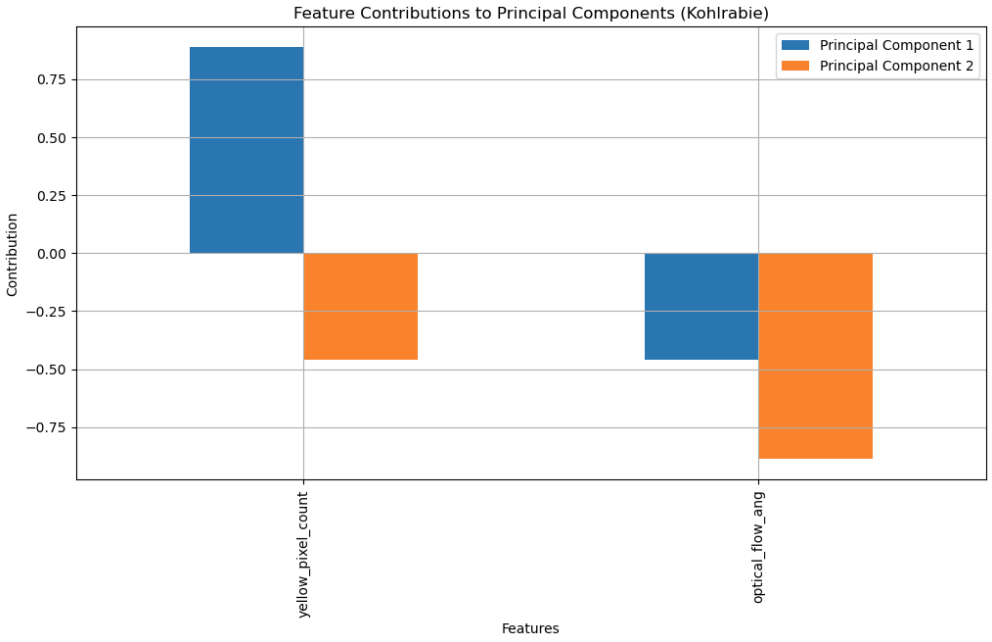

Figure 6.21: Feature Contribution to PCA from kohlrabi data

and optical_flow_ang being more significant for PC2.

The analysis of the dragoon lettuce, cucumber, and kohlrabi data using PCA provides valuable insight into the effectiveness and consistency of this method for distinguishing between sample groups. PCA successfully separates healthy from unhealthy samples for the dragoon lettuce data, highlighting the importance of features for further diagnostic or predictive modeling. In the cucumber data, yellow_pixel_count and optical_flow_ang are crucial for data separation, with yellow_pixel_count being more relevant for PC2 and optical_flow_ang for PC1. The kohlrabi data shows similar trends, with yellow_pixel_count being more significant for PC1 and optical_flow_ang for PC2.
Overall, the consistency of these findings across different datasets underscores the robustness of PCA in feature extraction and data separation, making it a reliable tool for diagnostic and predictive modeling tasks in various contexts. Given the repeated significance of the yellow_pixel_count and optical_flow_ang features, we will focus on these two features for future analyses and modeling efforts, as they have proven to be the most significant across all data.

6.2.3 Anomaly Detection

This section will explain the results of the change point detection. First, a classification comparison based on the LOF results on the data from the three species will be made. Following this, the results of detecting the point at which stress affects the plant will be shown and analyzed visually.

This study used the LOF algorithm to detect plant stress based on the features yellow_pixel_count and the optical_flow_ang. The data encompasses three plant species: kohlrabi, dragon lettuce, and cucumber. To facilitate a comparable analysis, an equal number of healthy and unhealthy test data were selected for all species. Since the training process also requires data, the smallest dataset determines the number of test data used. Consequently, four healthy time series were utilized for the training data, while the test data comprised four healthy and four unhealthy time series for each species. As part of this thesis, a request was made to a researcher who intermittently monitored the growth of the plants to create ground-truth data to determine the point at which plant stress is detected[1]. However, due to a miscommunication, the created data could not be effectively utilized, and a comparison between humans and machines could not be made.

The algorithm's performance was evaluated using confusion matrices for each species. The confusion matrix for the lettuce data in Figure 6.22 (a) shows that the LOF algorithm achieved perfect classification. All healthy plants were correctly identified as healthy TN, and all stressed plants were correctly classified as stressed TP. There were no false positives or false negatives. This proves that the traits of lettuce plants are distinguishable between stressed and healthy states, and the algorithm can effectively recognize these differences. The precision, recall and F1-score values are 1.00, 1.00, and 1.00, respectively. The small number of data points should be considered. While the results appear perfect, it is important to note that the algorithm would perform differently in a real, larger-scale scenario. A larger sample size is needed to validate the model's performance more robustly.

The confusion matrix for kohlrabi in Figure 6.22 (b) shows that three healthy plants were correctly identified as healthy TN. Two plants were incorrectly identified as stressed FP. All stressed plants were correctly identified as such TP, with no false negatives FN. These results demonstrate that the LOF algorithm can effectively detect stress in kohlrabi, although it occasionally misidentifies healthy plants as stressed. This is likely due to variability in the data or subtle differences in the yellow_pixel_count feature. The calculated precision, recall, and F1 scores are 0.67, 1.00, and 0.80, respectively. It is important to note that the small

[1]Unfortunately, the ground-truth data could not be used due to misunderstandings regarding the requirements.

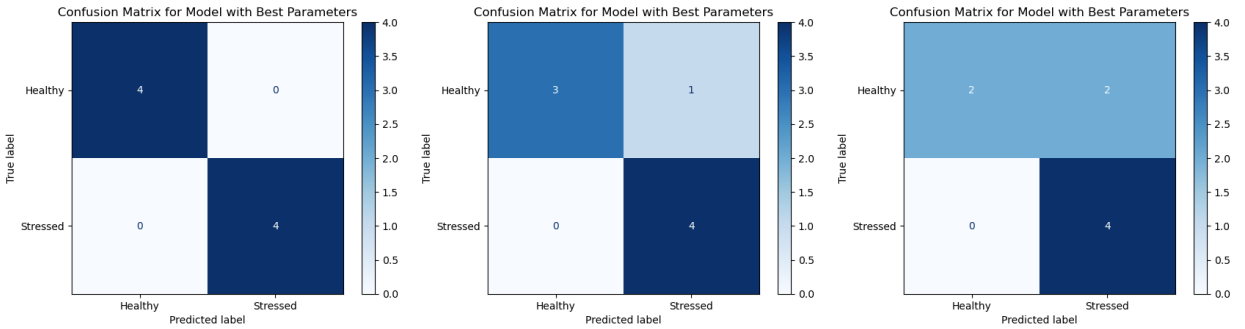

(a) (b) (c)

Figure 6.22: Confusion matrix of the (a) lettuce, (b) kohlrabi, (c) cucumber dataset

number of data points may bias the results. With only four healthy and stressed plants, individual misclassifications can significantly affect the calculated metrics. Therefore, these results should be interpreted cautiously, as they may need to be more representative of larger or more diverse data sets.

The confusion matrix for cucumber in Figure 6.22 (c) shows that of the healthy plants, two were correctly identified as healthy TN, while two were incorrectly classified as stressed FP. All stressed plants were correctly identified as TP, with no false negatives FN. The LOF algorithm performs well overall, but there are some misclassifications among the healthy plants. These are likely due to the same reasons as the kohlrabi data. The calculated precision, recall, and F1-score values are 0.75, 1.00, and 0.86, respectively. As with the other datasets, the small number of data points may skew the results. However, the impact of individual misclassifications on the calculated metrics is small, and the results are, therefore, reliable.

The LOF algorithm has proven effective in detecting stress in plants. The analysis of lettuce plants achieved perfect classification results, while some misclassifications occurred for kohlrabi and cucumber. Further investigations and adjustments are crucial to improve the accuracy and reliability of the algorithm. In particular, examining the causes of misclassifications and adjusting the feature selection or hyperparameters of the algorithm will lead to significant improvements. This study demonstrates that the LOF algorithm is an invaluable tool for detecting plant stress and can significantly enhance plant monitoring and care. The limited data set presents a challenge, but it also offers the opportunity to test and further develop the algorithm in smaller, controlled environments before applying it to larger data sets.

Following the discussion of the classification results, the detection accuracy of stress-induced

points will be presented. Initially, images of the four stressed and healthy plants for each species will be shown and discussed. Subsequently, a PCA of the eight-time series will be displayed, with all data before the detected stress point categorized as healthy and the remaining data categorized as stressed.

The Figure 6.23 consists of eight plots displaying time series data of yellow pixel counts for various lettuce plants. The top row represents healthy plants, while the bottom row represents stressed plants. A key focus of this analysis is to evaluate the accuracy and reliability of the detected change points used to identify plant stress.

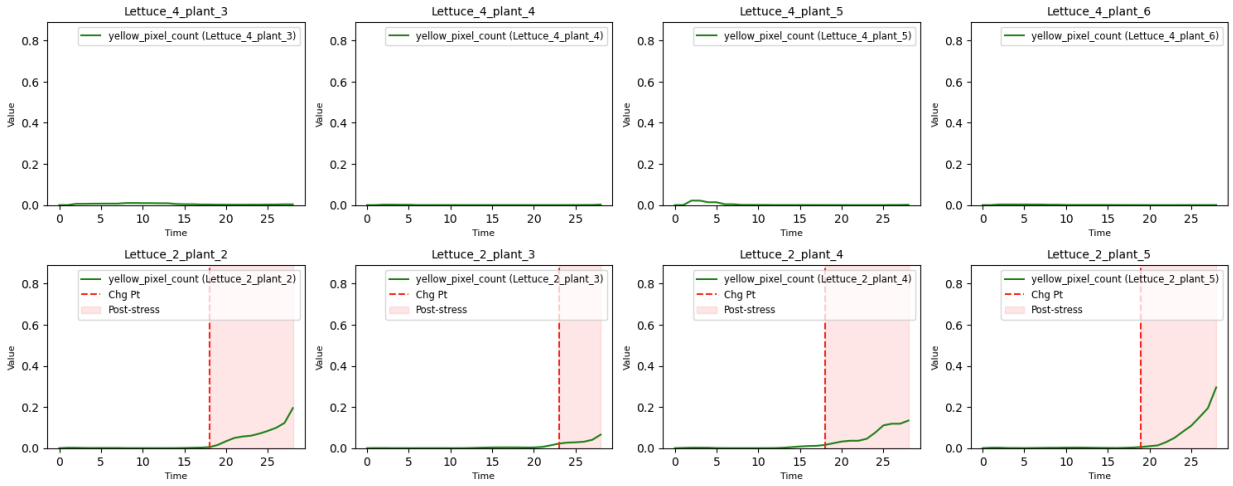

Figure 6.23: Time series plots of the yellow pixel count for eight different dragon lettuce plants, with four healthy plants in the top row and four unhealthy plants in the bottom row

In the plots of stressed plants in the bottom row, the change points (Chg Pt) are marked by red dashed lines, and the post-stress period is shaded in red. These markers are crucial for identifying the time the plants start showing visible stress symptoms, indicated by an increase in the yellow pixel count. The plot for Lettuce_2_plant_2 shows that the change point is detected around the 20th time unit. Following this point, there is a significant increase in the yellow pixel count, indicating a precise detection of the onset of stress. The substantial rise in the post-stress period confirms the accuracy of this change point. A similar pattern is observed for Lettuce_2_plant_3, where the change point is set around the 25th time unit. Here, a significant increase in yellow pixel count follows, suggesting that the change point accurately identifies the start of the stress condition. For Lettuce_2_plant_4, the change point is detected around the 15th time unit. After this point, a steady increase in the yellow pixel count is observed, indicating a reliable detection of the beginning of stress. The post-stress period shows a clear and significant increase in yellow pixels. Similarly,

Lettuce_2_plant_5 shows a change point around the 20th time unit. Following this point, there is a significant increase in the yellow pixel count, underscoring the accuracy of the detected change point. The plots of healthy plants in the top row show no change points, which is accurate since these plants did not experience stress, and the yellow pixel count remains consistently low. The accuracy of the change points can be assessed based on several criteria: The change points' temporal precision is high, as they are set precisely at the time when a noticeable increase in the yellow pixel count begins. This demonstrates the detection method's high temporal precision. The consistency of the data is noteworthy. After the change point, a clear and continuous increase in the yellow pixel count is observed in all stressed plants, confirming the change points' consistency in detecting stress. The marked increase in yellow pixel count after the change points during the post-stress period highlights the reliability of the detection method in identifying stress symptoms.
The Figure 6.24 displays the PCA analysis for dragoon lettuce, similar to the Figure 6.16. The axes are labeled as before, with "Principal Component 1" and "Principal Component 2." The data points are categorized into three groups: "Healthy" (small green circles), "Unhealthy Segment 1" (slightly larger green circles), and "Unhealthy Segment 2" (red crosses). The change points, marked by large red circles with black outlines, are primarily located within the "Unhealthy Segment 2" clusters. This placement indicates that the detection of stress moments in the plants is precise for the dragoon lettuce data. The change points mark areas where the plants experience significant stress, demonstrating a high stress detection accuracy.
Overall, the Figure 6.23 and Figure 6.24 demonstrate that the method for detecting change points in identifying stress in lettuce plants is both precise and reliable. The change points accurately mark the onset of stress symptoms, as confirmed by the significant increase in yellow pixel count during the post-stress period. This visual representation supports the method's effectiveness and is useful for early detection and monitoring of plant health through non-invasive imaging techniques.

The provided figure consists of eight plots displaying the time series data of yellow pixel counts for various cucumber plants. The top row represents healthy plants, while the bottom row shows stressed plants. Each plot includes a line indicating the number of yellow pixels over time. In the stressed plant plots, change points (Chg Pt) are marked by red dashed lines, and the post-stress period is shaded in red. The objective of this analysis is to evaluate the accuracy of the detected change points in identifying stress in the plants.
In the top row, which shows the healthy plants, the yellow pixel count remains consistently

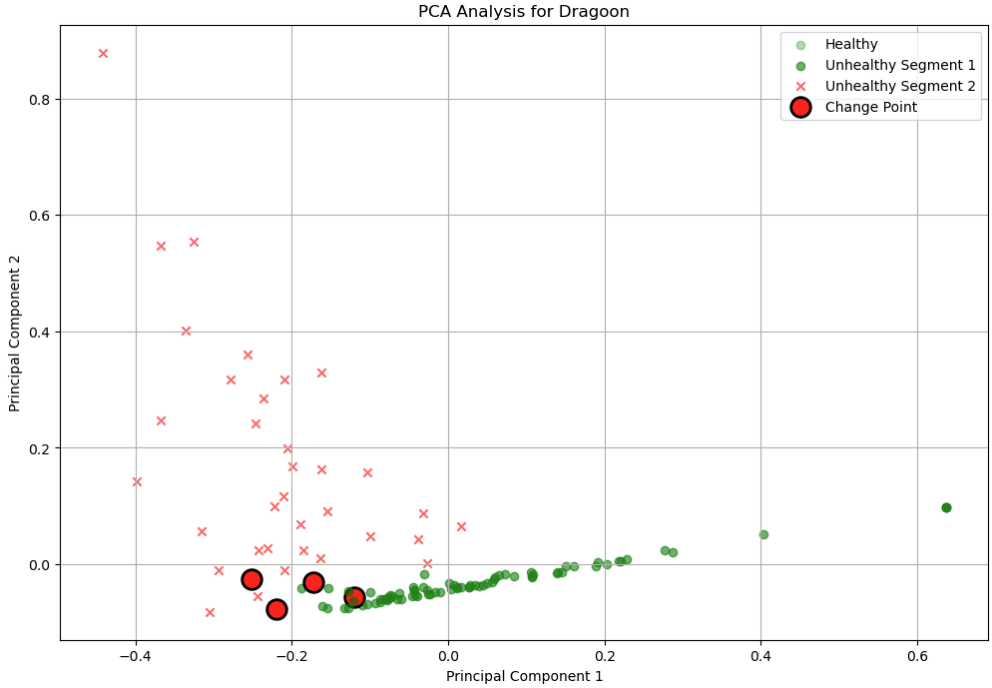

Figure 6.24: PCA Analysis for lettuce dragoon, illustrating change points (red circles) identifying the onset of plant stress

low throughout the observation period. In the plot for Cucumber_4_Left, the yellow pixel count remains low throughout, indicating no significant changes in the plant's condition, suggesting the plant remains healthy. For Cucumber_9_Right, the yellow pixel count remains stable and low for most of the observation period despite being labeled as stressed. A change point is detected around the 90th time unit, after which there is a slight increase, but it remains relatively stable. Cucumber_9_Left also shows a low and stable yellow pixel count with minor fluctuations, indicating a healthy state without significant stress. In the plot for Cucumber_10_Right, the yellow pixel count stays relatively stable until a change point is detected around the 100th time unit. After this point, there is a notable increase, suggesting the onset of stress.

A clearer pattern emerges in the bottom row, which represents stressed plants. Cucumber_3_Right shows a change point around the 50th time unit. Following this point, the yellow pixel count significantly increases and fluctuates but remains elevated, indicating a period of stress. Cucumber_3_Left exhibits a similar pattern to Cucumber_3_Right, with a change point around the 50th time unit and a marked increase in yellow pixel count, confirming the onset of stress. Cucumber_7_Right maintains a low and stable yellow pixel count until about the 100th time unit. After the change point, there is a noticeable in-

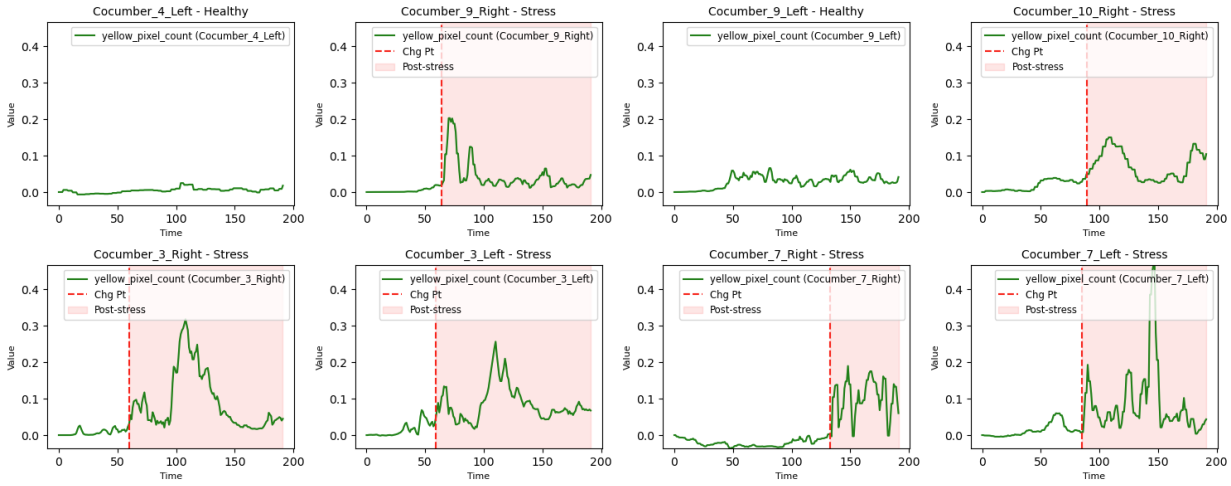

Figure 6.25: Time series plots of the yellow pixel count for eight different cucumber plants, with multiple stressed plants marked red

crease, indicating that the plant is experiencing stress. For Cucumber_7_Left, the change point is detected around the 100th time unit. Following this point, there is a significant and sustained increase in yellow pixel count, highlighting the stress period.

The accuracy of the change points can be evaluated based on several factors. First, the temporal precision of the change points is high, as they are set precisely at the time when noticeable changes in the yellow pixel count occur. This demonstrates high temporal precision in detecting the onset of stress. Second, the consistency of the data is noteworthy, as a clear and continuous increase in yellow pixel count is observed in all stressed plants after the change point. This consistency confirms the reliability of the change point detection in identifying stress. Third, the substantial increase in yellow pixel count during the post-stress period in stressed plants underscores the method's effectiveness in detecting stress symptoms.

The Figure 6.26 shows the PCA analysis for cucumber by separating the stressed timelines by the detected change points. The data points are similarly grouped: "Healthy" (small green circles), "Unhealthy Segment 1" (slightly larger green circles), and "Unhealthy Segment 2" (red crosses). The plot is densely populated with data points, especially around the origin. The change points, marked by large red circles with black outlines, are distributed within the "Unhealthy Segment 2" clusters. Despite the overlap between healthy and unhealthy states, the change points precisely indicate the moment the plants experience stress. This suggests that stress detection is accurate even in a more complex and densely populated data space. Additionally, Figure 6.25 and Figure 6.26 demonstrate that the change point detection

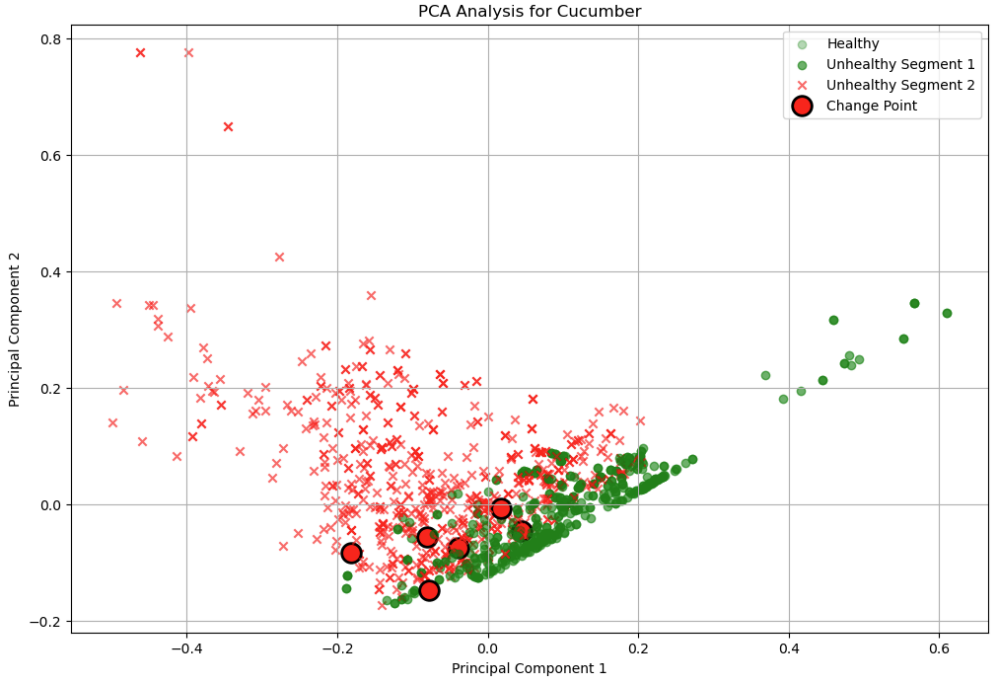

Figure 6.26: PCA Analysis for cucumber, illustrating change points (red circles) identifying the onset of plant stress

method for identifying stress in cucumber plants is both precise and reliable, similar to the results observed in the dragon lettuce dataset. The yellow pixel count remains low and stable in healthy plants, while in stressed plants, a significant increase follows the detected change points. This visual representation confirms the method's effectiveness and is valuable for early detection and monitoring of plant health through non-invasive imaging techniques. The detection of change points allows for the timely identification of stress, providing an essential tool for maintaining plant health.

The provided figure consists of eight plots displaying the time series data of yellow pixel counts for various kohlrabi plants. The top row represents healthy plants, while the bottom shows stressed plants. Each plot includes a line indicating the number of yellow pixels over time. Change points (Chg Pt) are marked by red dashed lines in the stressed plant plots, and the post-stress period is shaded in red. The objective of this analysis is to evaluate the accuracy of the detected change points in identifying stress in the plants.
In the top row, which shows the healthy plants, the yellow pixel count remains consistently low throughout the observation period. In the plot for Kohlrabi_5_Right, the yellow pixel count remains low and stable, indicating no significant changes in the plant's condition, sug-

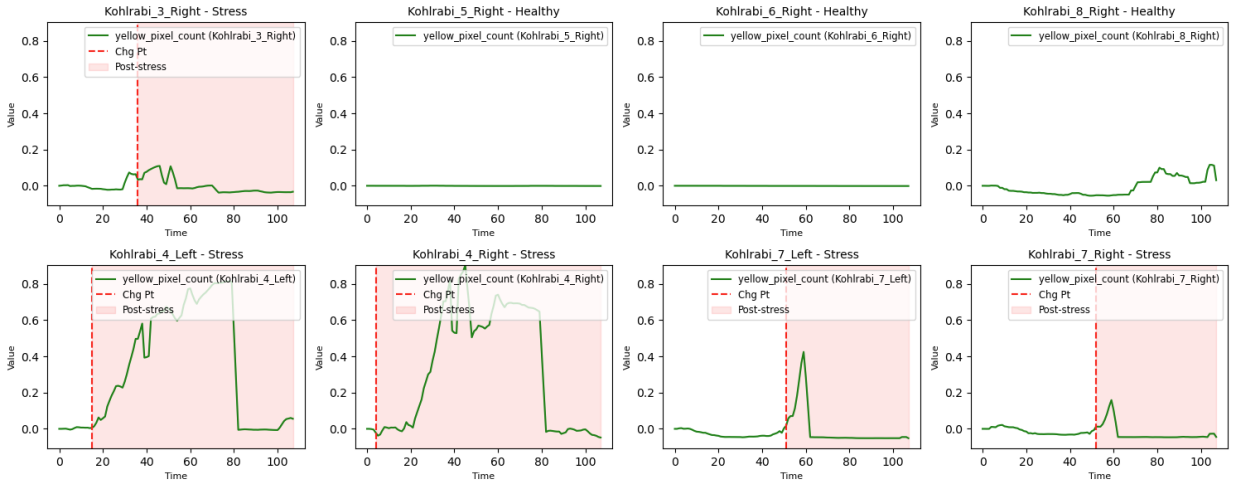

Figure 6.27: Time series plots of the yellow pixel count for eight different dragon lettuce plants, with multiple stressed plants marked red

gesting the plant remains healthy. Similarly, Kohlrabi_6_Right exhibits a consistently low yellow pixel count, showing no significant fluctuations and indicating a healthy state. In the case of Kohlrabi_8_Right, the yellow pixel count remains low for most of the observation period, with only minor increases toward the end, but these do not indicate significant stress. The plot for Kohlrabi_3_Right shows a change point around the 40th time unit, followed by a slight increase in yellow pixel count, but it remains relatively stable, suggesting minimal stress. A more apparent pattern emerges in the bottom row, representing stressed plants. Kohlrabi_4_Left shows a change point around the 40th time unit. Following this point, there is a significant increase in the yellow pixel count, which then fluctuates but remains elevated, indicating a period of stress. Kohlrabi_4_Right displays a similar pattern, with a change point around the 40th time unit followed by a marked increase in yellow pixel count, confirming the onset of stress. The plot for Kohlrabi_7_Left shows a low and stable yellow pixel count until about the 60th time unit. After the change point, there is a noticeable increase, indicating that the plant is experiencing stress. Similarly, Kohlrabi_7_Right shows a change point around the 60th time unit, followed by a significant increase in yellow pixel count, highlighting the stress period. The accuracy of the change points can be evaluated based on several factors: The change points' temporal precision is high, as they are set precisely at the time when noticeable changes in the yellow pixel count occur. This demonstrates high temporal precision in detecting the onset of stress. The consistency of the data is noteworthy, as a clear and continuous increase in yellow pixel count is observed in all stressed plants after the change point. This consistency confirms the reliability of the change

point detection in identifying stress. The substantial increase in yellow pixel count during the post-stress period in stressed plants underscores the method's effectiveness in detecting stress symptoms.

The Figure 6.28 shows the PCA analysis for kohlrabi data. The distribution of data points seems to indicate some separation between healthy (small green circles) and unhealthy states (red crosses). The change points, marked by large red circles with black outlines, appear to be placed within the "Unhealthy Segment 2" clusters, suggesting potential moments when the plants might experience stress. However, the separation of data points is not entirely distinct, making the accuracy of stress detection less certain in this case.

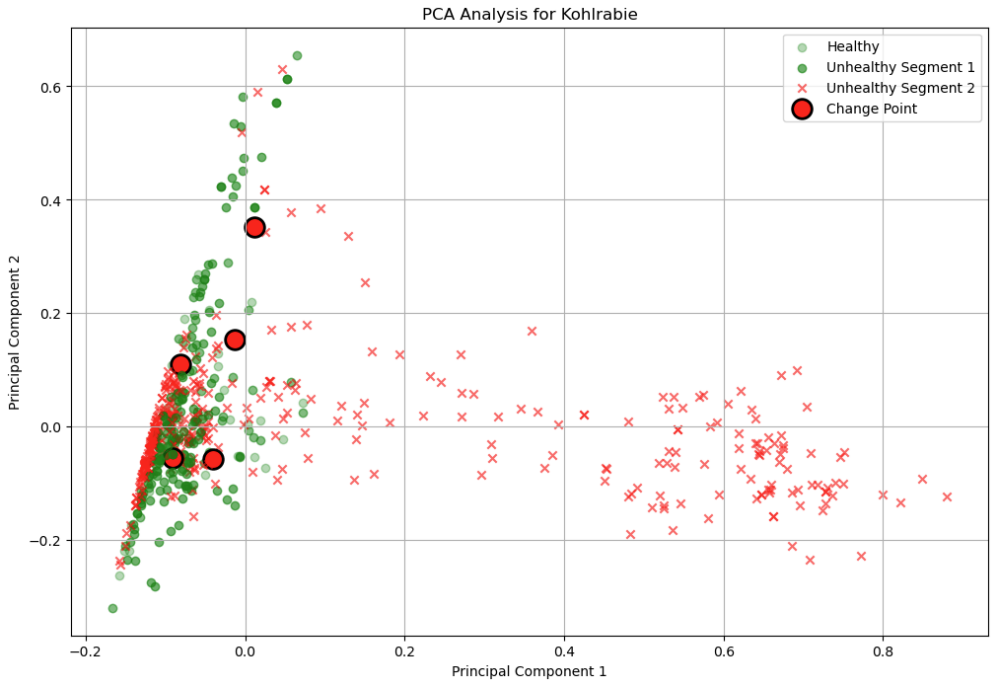

Figure 6.28: PCA Analysis for kohlrabi, illustrating change points (red circles) identifying the onset of plant stress

Therefore, the Figure 6.27 and Figure 6.28 indicate that the method for detecting change points in identifying stress in kohlrabi plants is moderately precise and reliable. While the yellow_pixel_count generally remains low and stable in healthy plants, the increase in stressed plants following the detected change points is not always significant. This visual representation raises some doubts about the method's overall effectiveness for early detection and monitoring of plant health through non-invasive imaging techniques. Identifying change points offers some potential for recognizing stress, but its reliability for maintaining plant health needs to be investigated.

This section provided for lettuce, cucumber, and kohlrabi plants collectively demonstrates that the method for detecting change points in identifying plant stress is both precise and reliable. In each case, the change points accurately mark the onset of stress symptoms, as evidenced by a significant increase in yellow pixel count during the post-stress period. This consistent pattern across different plant types underscores the method's effectiveness in distinguishing between healthy and stressed plants. However, noting instances of falsely detected change points is also important. In some cases, change points were identified in plants that remained stable and healthy, indicating that while the method is generally effective, there is room for improvement in reducing false positives. Overall, the ability to accurately detect change points allows for the timely identification of stress, providing an essential tool for early intervention and monitoring of plant health through non-invasive imaging techniques. This approach ultimately aids in maintaining plant health, improving crop management, and potentially enhancing yield outcomes.

7 Discussion

This study uses the EDEN ISS dataset to investigate methods for detecting abiotic stress in plants. The goal was to develop algorithms for image preprocessing, identify key features for stress detection, and implement suitable methods for anomaly detection. The focus was on developing robust and efficient approaches for analyzing plant health in controlled environments, particularly concerning their application in space missions.

A central finding of the investigation was the identification of the number of yellow pixels and the optical flow angle as key features for stress detection. These features proved effective in distinguishing between healthy and stressed plants. The Green Threshold method for plant segmentation was efficient, providing reliable results with minimal computational effort. Similarly, the LOF method demonstrated accuracy and reliability in anomaly detection, effectively identifying the onset of stress in plants.

Despite these promising results, the study has several limitations. The current methodology for plant segmentation showed weaknesses in detecting overlapping plants and inaccurate tray detection. The Green Threshold method must be adjusted for more precise segmentation, particularly for every plant and every environment. Additionally, it would be beneficial to re-test the SAM and create markers to improve segmentation and reduce dependence on specific markers.

Another critical point is the need for more accurate and frequent data collection. Hourly data captures help better track plant movements and provide a larger dataset for analysis. This would improve the detection of stress moments and increase model accuracy.

Moreover, extensive tests with ground-truth data should be compared with human assessments to determine who detects stress earlier. Such comparisons are crucial for validating the effectiveness and reliability of the developed methods.

Using yellow_pixel_count and optical_flow_ang as features proved helpful for stress detection in some plant species; however, it can lead to errors in others, such as cucumbers with yellow flowers or tomatoes where older leaves turn brown. These natural color changes can distort stress detection and lead to false alarms. Therefore, further refining this method or integrating additional features is necessary to improve stress detection accuracy.

Although the LOF method showed high accuracy for anomaly detection, its reliability could be affected by different environmental conditions and plant growth stages. Future studies should test the robustness of this method under various conditions and improve its adaptability to different plant species and environmental conditions. Additionally, the LOF method's classification accuracy and change point detection capabilities need to be examined more closely. The ability to accurately classify plants as stressed or healthy and to detect the exact points at which stress occurs is critical for timely interventions. Therefore, it is essential to validate the LOF method's performance in classification and change point detection under various conditions to ensure its effectiveness across different scenarios.

8 Conclusion and Outlook

This final chapter summarizes the primary findings and reflects on the research questions and objectives. Additionally, it provides insights into potential future developments and applications, highlighting areas where further research and innovation could enhance the current understanding and practice of plant stress detection.

This study aimed to develop and validate methods for detecting abiotic stress in plants using the EDEN ISS dataset. The primary objectives were to develop algorithms for image preprocessing, identify key features for stress detection, and implement suitable methods for anomaly detection. These objectives were successfully achieved, providing significant insights and practical contributions.

A central finding was identifying the number of yellow pixels and the optical flow angle as key features for stress detection. These features proved effective in distinguishing between healthy and stressed plants. The Green Threshold method for plant segmentation was efficient, providing reliable results with minimal computational effort. Similarly, the LOF method demonstrated high accuracy and reliability in anomaly detection, effectively identifying the onset of stress in plants, as evidenced by high precision, recall, and F1 scores. These results underscore the importance of selecting appropriate features and methods for plant stress detection. The number of yellow pixels and the optical flow angle were identified as robust indicators of plant health, providing a reliable basis for stress detection. Overall, the Green Threshold and LOF methods were validated as practical tools for analyzing plant health in controlled environments.

This work contributes to the broader field of agriculture in controlled environments, particularly in the context of space missions. Accurately detecting plant stress is crucial for the success of long-duration space missions, where reliable food production systems are essential. The developed and validated methods offer practical solutions for monitoring plant health and ensuring the sustainability of agricultural systems in extreme environments. Addressing the need for reliable stress detection methods contributes to advancing sustainable agricultural practices in extreme environments, including space. The findings and methods developed provide a solid foundation for future research and innovation, paving the way for

more resilient and efficient agricultural systems.
The integration of advanced technologies, interdisciplinary collaboration, and the continuous refinement of methods will be essential to addressing plant stress detection challenges and ensuring the sustainability of agricultural systems in various and extreme environments.

Bibliography

[AA19] Asokan, Anju; Anitha, J.: Change detection techniques for remote sensing applications: a survey. Earth Science Informatics, 12(2):143–160, Jun 2019.

[AB16] Alwin, Duane F.; Beattie, Brett A.: The KISS Principle in Survey Design: Question Length and Data Quality. Sociological Methodology, 46(1):121–152, 2016.

[Ak19] Akiba, Takuya; Sano, Shotaro; Yanase, Toshihiko; Ohta, Takeru; Koyama, Masanori: Optuna: A Next-generation Hyperparameter Optimization Framework. In: Proceedings of the 25th ACM SIGKDD International Conference on Knowledge Discovery & Data Mining. KDD '19, Association for Computing Machinery, New York, NY, USA, p. 2623–2631, 2019.

[Al21] Alghushairy, Omar; Alsini, Raed; Soule, Terence; Ma, Xiaogang: A Review of Local Outlier Factor Algorithms for Outlier Detection in Big Data Streams. Big Data and Cognitive Computing, 5(1), 2021.

[Ar16] Araya, Daniel B.; Grolinger, K.; ElYamany, Hany F.; Capretz, Miriam A. M.; Bitsuamlak, G.: Collective contextual anomaly detection framework for smart buildings. In: 2016 International Joint Conference on Neural Networks (IJCNN). pp. 511–518, 2016.

[Ar18] Araus, José Luis; Kefauver, Shawn C.; Zaman-Allah, Mainassara; Olsen, Mike S.; Cairns, Jill E.: Translating High-Throughput Phenotyping into Genetic Gain. Trends in Plant Science, 23(5):451–466, 2018.

[BBS22] Benkő, Zsigmond; Bábel, Tamás; Somogyvári, Zoltán: Model-free detection of unique events in time series. Scientific Reports, 12(1):227, Jan 2022.

[BEK19] Bassine, Fatima Zahra; Errami, Ahmed; Khaldoun, Mohammed: Vegetation Recognition Based on UAV Image Color Index. In: 2019 IEEE International

Conference on Environment and Electrical Engineering and 2019 IEEE Industrial and Commercial Power Systems Europe (EEEIC / ICPS Europe). pp. 1–4, 2019.

[BG21] Bhoopander Giri, Mahaveer Prasad Sharma: Plant Stress Biology. Springer, 2021.

[Bh20] Bhandari, Mahendra; Ibrahim, Amir M.H.; Xue, Qingwu; Jung, Jinha; Chang, Anjin; Rudd, Jackie C.; Maeda, Murilo; Rajan, Nithya; Neely, Haly; Landivar, Juan: Assessing winter wheat foliage disease severity using aerial imagery acquired from small Unmanned Aerial Vehicle (UAV). Computers and Electronics in Agriculture, 176:105665, 2020.

[BSA09] Börner, Horst; Schlüter, Klaus; Aumann, Jens: Abiotische Schadursachen. In: Pflanzenkrankheiten und Pflanzenschutz. Springer Berlin Heidelberg, Berlin, Heidelberg, pp. 13–22, 2009.

[CA79] Coleman, G.B.; Andrews, H.C.: Image segmentation by clustering. Proceedings of the IEEE, 67(5):773–785, 1979.

[Ce90] Celenk, Mehmet: A color clustering technique for image segmentation. Computer Vision, Graphics, and Image Processing, 52(2):145–170, 1990.

[Da19] Dada, Emmanuel Gbenga; Bassi, Joseph Stephen; Chiroma, Haruna; Abdulhamid, Shafi'i Muhammad; Adetunmbi, Adebayo Olusola; Ajibuwa, Opeyemi Emmanuel: Machine learning for email spam filtering: review, approaches and open research problems. Heliyon, 5(6):e01802, 2019.

[DCSA19] Das Choudhury, Sruti; Samal, Ashok; Awada, Tala: Leveraging Image Analysis for High-Throughput Plant Phenotyping. Frontiers in Plant Science, 10, 2019.

[DMC15] Dhanachandra, Nameirakpam; Manglem, Khumanthem; Chanu, Yambem Jina: Image Segmentation Using K -means Clustering Algorithm and Subtractive Clustering Algorithm. Procedia Computer Science, 54:764–771, 2015. Eleventh International Conference on Communication Networks, ICCN 2015, August 21-23, 2015, Bangalore, India Eleventh International Conference on Data Mining and Warehousing, ICDMW 2015, August 21-23, 2015, Bangalore, India Eleventh International Conference on Image and Signal Processing, ICISP 2015, August 21-23, 2015, Bangalore, India.

[Ga23] Gao, Shanghua; Li, Zhong-Yu; Yang, Ming-Hsuan; Cheng, Ming-Ming; Han, Junwei; Torr, Philip: Large-Scale Unsupervised Semantic Segmentation. IEEE Transactions on Pattern Analysis and Machine Intelligence, 45(6):7457–7476, 2023.

[GDD22] Ghosal, Daipayan; Das, Arunita; Dhal, Krishna Gopal: A Comparative Study among Clustering Techniques for Leaf Segmentation in Rosette Plants. Pattern Recognition and Image Analysis, 32(1):129–141, Mar 2022.

[Ge21] Geldhof, Batist; Pattyn, Jolien; Eyland, David; Carpentier, Sebastien; Van de Poel, Bram: A digital sensor to measure real-time leaf movements and detect abiotic stress in plants. Plant Physiology, 187(3):1131–1148, 08 2021.

[Gi21] Giovos, Rigas; Tassopoulos, Dimitrios; Kalivas, Dionissios; Lougkos, Nestor; Priovolou, Anastasia: Remote Sensing Vegetation Indices in Viticulture: A Critical Review. Agriculture, 11(5), 2021.

[Gi22] Gill, Taqdeer; Gill, Simranveer K.; Saini, Dinesh K.; Chopra, Yuvraj; de Koff, Jason P.; Sandhu, Karansher S.: A Comprehensive Review of High Throughput Phenotyping and Machine Learning for Plant Stress Phenotyping. Phenomics, 2(3):156–183, Jun 2022.

[Go08] Gonzalez, Rafael C: Digital image processing. Pearson education, 2008.

[GSL22] Galviz, Yutcelia; Souza, Gustavo M.; Lüttge, Ulrich: The biological concept of stress revisited: relations of stress and memory of plants as a matter of space–time. 2022.

[HC15] Hayes, Michael A.; Capretz, Miriam AM: Contextual anomaly detection framework for big sensor data. Journal of Big Data, 2(1):2, Feb 2015.

[He22] Heldmann, Jennifer L.; Marinova, Margarita M.; Lim, Darlene S.S.; Wilson, David; Carrato, Peter; Kennedy, Keith; Esbeck, Ann; Colaprete, Tony Anthony; Elphic, Richard C.; Captain, Janine; Zacny, Kris; Stolov, Leo; Mellerowicz, Boleslaw; Palmowski, Joseph; Bramson, Ali M.; Putzig, Nathaniel; Morgan, Gareth; Sizemore, Hanna; Coyan, Josh: Mission Architecture Using the SpaceX Starship Vehicle to Enable a Sustained Human Presence on Mars. New Space, 10(3):259–273, 2022. PMID: 36199953.

[HG15] Hira, Zena M.; Gillies, Duncan F.: A Review of Feature Selection and Feature Extraction Methods Applied on Microarray Data. Advances in Bioinformatics, 2015(1):198363, 2015.

[HL09] Hamarneh, Ghassan; Li, Xiaoxing: Watershed segmentation using prior shape and appearance knowledge. Image and Vision Computing, 27(1):59–68, 2009. Canadian Robotic Vision 2005 and 2006.

[JPW17] Jebb, Andrew T.; Parrigon, Scott; Woo, Sang Eun: Exploratory data analysis as a foundation of inductive research. Human Resource Management Review, 27(2):265–276, 2017.

[KB09] Kaganami, Hassana Grema; Beiji, Zou: Region-Based Segmentation versus Edge Detection. In: 2009 Fifth International Conference on Intelligent Information Hiding and Multimedia Signal Processing. pp. 1217–1221, 2009.

[Ki23] Kirillov, A.; Mintun, Eric; Ravi, Nikhila; Mao, Hanzi; Rolland, Chloe; Gustafson, Laura; Xiao, Tete; Whitehead, Spencer; Berg, A.; Lo, Wan-Yen; Dollár, Piotr; Girshick, Ross B.: Segment Anything. ArXiv, abs/2304.02643, 2023.

[Kr16] Krig, Scott: Computer Vision Metrics : Textbook Edition. Springer, 2016.

[Le20] Letzgus, S.: Change-point detection in wind turbine SCADA data for robust condition monitoring with normal behaviour models. Wind Energy Science, 5(4):1375–1397, 2020.

[Lu17] Luo, Yaozhong; Liu, Longzhong; Huang, Qinghua; Li, Xuelong: A Novel Segmentation Approach Combining Region- and Edge-Based Information for Ultrasound Images. BioMed Research International, 2017(1):9157341, 2017.

[Ma09] Mallapragada, Pavan Kumar; Jin, Rong; Jain, Anil K.; Liu, Yi: SemiBoost: Boosting for Semi-Supervised Learning. IEEE Transactions on Pattern Analysis and Machine Intelligence, 31(11):2000–2014, 2009.

[Me94] Meyer, Fernand: Topographic distance and watershed lines. Signal Processing, 38(1):113–125, 1994. Mathematical Morphology and its Applications to Signal Processing.

[Mi15] Minervini, Massimo; Fischbach, Andreas; Scharr, Hanno; Tsaftaris, Sotirios A.: Finely-grained annotated datasets for image-based plant phenotyping. Pattern Recognition Letters, pp. 1–10, 2015.

[Mi22] Mittal, Himanshu; Pandey, Avinash Chandra; Saraswat, Mukesh; Kumar, Sumit; Pal, Raju; Modwel, Garv: A comprehensive survey of image segmentation: clustering methods, performance parameters, and benchmark datasets. Multimedia Tools and Applications, 81(24):35001–35026, Oct 2022.

[Mo09] Morgenthaler, Stephan: Exploratory data analysis. WIREs Computational Statistics, 1(1):33–44, 2009.

[Pa12] Panigrahi, Prabin Kumar: A Comparative Study of Supervised Machine Learning Techniques for Spam E-mail Filtering. In: 2012 Fourth International Conference on Computational Intelligence and Communication Networks. pp. 506–512, 2012.

[Rh11] Rhew, Isaac C.; Vander Stoep, Ann; Kearney, Anne; Smith, Nicholas L.; Dunbar, Matthew D.: Validation of the Normalized Difference Vegetation Index as a Measure of Neighborhood Greenness. Annals of Epidemiology, 21(12):946–952, 2011.

[Sc16] Scharr, H.; Minervini, M.; French, A.; Klukas, Christian; Kramer, D.; Liu, Xiaoming; Luengo, Imanol; Pape, Jean-Michel; Polder, G.; Vukadinovic, Danijela; Yin, Xi; Tsaftaris, S.: Leaf segmentation in plant phenotyping: a collation study. Machine Vision and Applications, 27:585–606, 2016.

[Sc22] Schubert, Daniel: Highlights 2022 Yearly Status Report Planetary Infrastructures. 2022.

[Sc26] Schubert, Daniel: PHM Design Report. 2019-06-26.

[SD23] Sasmal, Buddhadev; Dhal, Krishna Gopal: A survey on the utilization of Superpixel image for clustering based image segmentation. Multimedia Tools and Applications, 82(23):35493–35555, Sep 2023.

[Sm20] Smith, Marshall; Craig, Douglas; Herrmann, Nicole; Mahoney, Erin; Krezel, Jonathan; McIntyre, Nate; Goodliff, Kandyce: The Artemis Program: An Overview of NASA's Activities to Return Humans to the Moon. In: 2020 IEEE Aerospace Conference. pp. 1–10, 2020.

[SNL19] Shewalkar, Apeksha; Nyavanandi, Deepika; Ludwig, Simone A.: Performance Evaluation of Deep Neural Networks Applied to Speech Recognition: RNN, LSTM and GRU. Journal of Artificial Intelligence and Soft Computing Research, 9(4):235–245, 2019.

[SQP02] Sural, S.; Qian, Gang; Pramanik, S.: Segmentation and histogram generation using the HSV color space for image retrieval. In: Proceedings. International Conference on Image Processing. volume 2, pp. II–II, 2002.

[SS19] Schmidt, Maximilian; Simic, Marko: , Normalizing flows for novelty detection in industrial time series data, 2019.

[St21] Stutsel, Bonny; Johansen, Kasper; Malbéteau, Yoann M.; McCabe, Matthew F.: Detecting Plant Stress Using Thermal and Optical Imagery From an Unoccupied Aerial Vehicle. Frontiers in Plant Science, 12, 2021.

[Te10] Teng, Mingyan: Anomaly detection on time series. In: 2010 IEEE International Conference on Progress in Informatics and Computing. volume 1, pp. 603–608, 2010.

[WMB23] Williams, Dominic; Macfarlane, Fraser; Britten, Avril: Leaf Only SAM: A Segment Anything Pipeline for Zero-Shot Automated Leaf Segmentation. ArXiv, abs/2305.09418, 2023.

[Ya20] Yang, Jiawei: Outlier detection techniques. PhD thesis, Itä-Suomen yliopisto, 2020.

[Za20] Zabel, Paul; Zeidler, Conrad; Vrakking, Vincent; Dorn, Markus; Schubert, Daniel: Biomass Production of the EDEN ISS Space Greenhouse in Antarctica During the 2018 Experiment Phase. Frontiers in Plant Science, 11, 2020.

[Ze19] Zeidler, Conrad; Zabel, Paul; Vrakking, Vincent; Dorn, Markus; Bamsey, Matthew; Schubert, Daniel; Ceriello, Antonio; Fortezza, Raimondo; De Simone, Domenico; Stanghellini, Cecilia; Kempkes, Frank; Meinen, Esther; Mencarelli, Angelo; Swinkels, Gert-Jan; Paul, Anna-Lisa; Ferl, Robert J.: The Plant Health Monitoring System of the EDEN ISS Space Greenhouse in Antarctica During the 2018 Experiment Phase. Frontiers in Plant Science, 10, 2019.

[ZIE17] Zhang, Richard; Isola, Phillip; Efros, Alexei A.: Split-Brain Autoencoders: Unsupervised Learning by Cross-Channel Prediction. In: 2017 IEEE Conference on Computer Vision and Pattern Recognition (CVPR). pp. 645–654, 2017.

[Zo16] Zorn, Wilfried; Marks, Gerhard; Heß, Hubert; Bergmann, Werner: Erkennen von Ernährungsstörungen bei Kulturpflanzen. In: Handbuch zur visuellen Diagnose von Ernährungsstörungen bei Kulturpflanzen. Springer Berlin Heidelberg, Berlin, Heidelberg, 2016.

Appendix

Content of the online folder

Folder directory	Files	Description
\masterthesis	masterthesis_Nordmann.pdf \masterthesis_Source	The masterthesis in Portable Document Format (PDF) The LaTeX source files of the bachelor thesis
\Source_Code	\dataset \plant_stress_detection_system	EDEN ISS dataset Folder with the components and the csv files for executing intermediate steps

Table 8.1: Content of the folder

Diagnosis topic to recognize the cause of nutrient deficiency

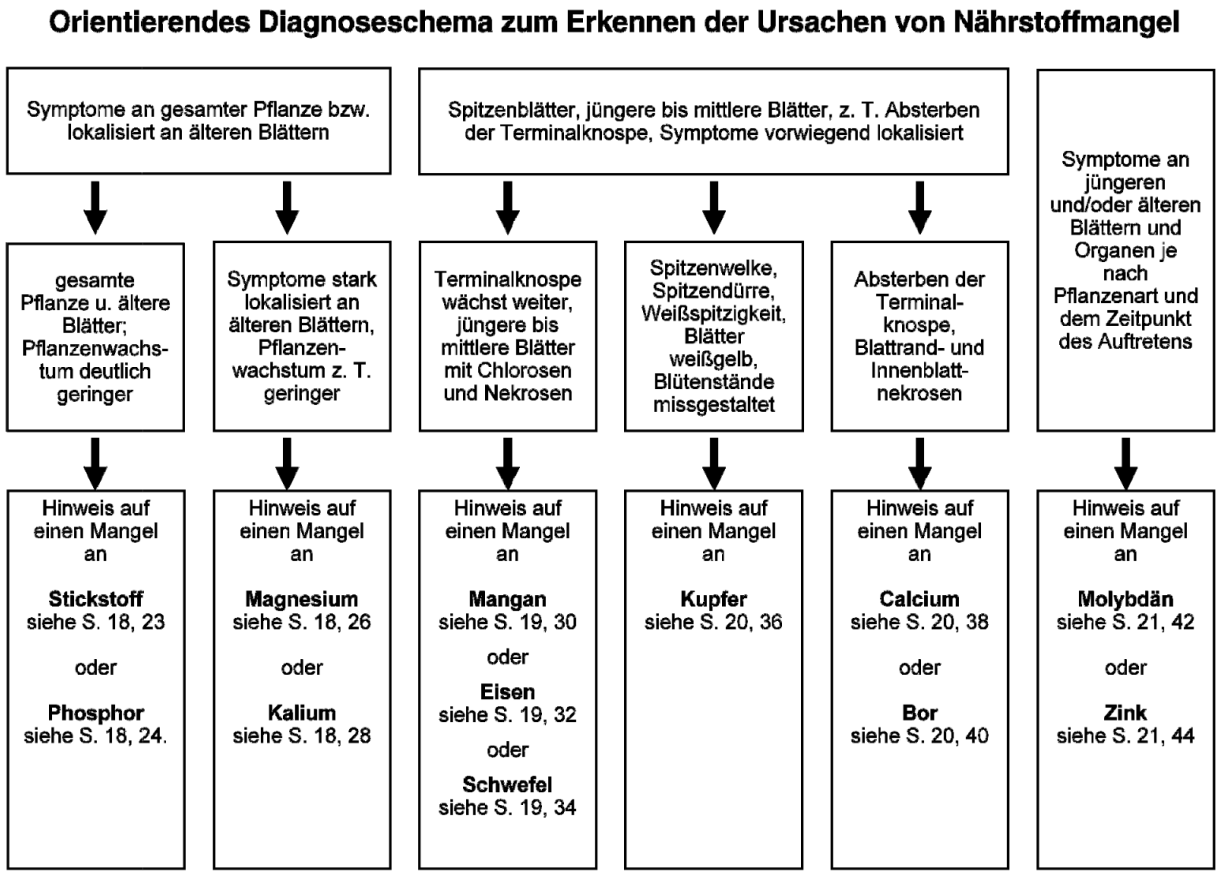

Figure 8.1: Causes of nutrient deficiency [Zo16]

Labeled table of plant stress images

Table 8.2: Labeled Plant Stress Images

File	Crop	Stress
HDCam_L4-1L_ 20190918_2358.jpeg HDCam_L4-1L_ 20200215_2358.jpeg HDCam_L4-1L_ 20200314_2358.jpeg HDCam_L4-1R_ 20190809_2358.jpeg	'Dragoon' lettuce	The grey/black marks in the center of the plant is caused by what's called calcium tip burn. This happens when the plant grows so quickly that it can't get enough calcium to the edges of the leaves fast enough. This affects the new leaves of a plant. This causes the cells at the edges of the leaves to not divide properly, causing this burning to appear and for the edges of the leaves to not unfurl properly. This is not an issue related to the amount of calcium in the nutrient solution, but rather that the plant is growing faster than the rate at which it can allocate calcium. The best way to avoid this is to choose cultivars that are not as susceptible to this. We see calcium tip burn with 'Dragoon' lettuce in other systems, and it is common in other crops we may work with such as strawberry. In addition, there is some yellowing around the edges of the older leaves of these lettuce plants. This could be from a number of causes, so we can't definitively say what from the photos alone. Please note that neither calcium tip burn nor the yellowing mean that the plants shouldn't be eaten. There are some other issues that can arise from these symptoms, but the burned and yellow edges can be cut off of the leaves, the remainder of which can be eaten.
HDCam_R1-2C_ 20180518_2358.jpeg HDCam_R1-2C_ 20181022_2358.jpeg	orange cherry tomato	The dried debris is simply old leaves and stems that need to be removed. This is normal for this crop.
HDCam_R1-2C_ 20200426_2358.jpeg HDCam_R1-2C_ 20200624_2358.jpeg HDCam_R1-2C_ 20200915_2358.jpeg	kohlrabi	Magnesium deficiency, at the very least. May have other nutrient stress, but this is the most prominent.
HDCam_R1-4C_ 20180520_2358.jpeg	orange cherry tomato	The dried debris is simply old leaves and stems that need to be removed. This is normal for this crop. It looks like a wilting event also occurred prior to when this photo was taken, although we would need to see a log book to of greenhouse events to confirm.
HDCam_R2-4C_ 20180518_2358.jpeg HDCam_R2-4C_ 20181031_2358.jpeg	red cherry tomato	The dried debris is simply old leaves and stems that need to be removed. This is normal for this crop. There are also a few leaves with symptoms of nutrient stress, although it is difficult to determine more precisely what nutrient(s).
HDCam_R3-4C_ 20190816_2358.jpeg HDCam_R3-4C_ 20200930_2358.jpeg	cucumber	The yellowing around the edges of the leaves is likely from potassium deficiency. Other leaves indicate that there may be additional nutrient deficiency, but the symptoms are nonconclusive. The lower leaves that are brown are either old leaves that need to be removed, or there could have been a previous stress event, such as a wilting event, that caused premature leaf death. We would need more information about the events prior to when these photos were taken to make more definitive conclusions.

Eidesstattliche Erklärung

Hiermit erkläre ich an Eides statt, dass ich die vorliegende Arbeit selbständig und ohne fremde Hilfe angefertigt habe. Die aus fremden Quellen direkt oder indirekt übernommenen Gedanken sind als solche einzeln kenntlich gemacht. Es wurden keine anderen als die angegebenen Quellen und Hilfsmittel benutzt. Die Arbeit wurde bisher keiner anderen Prüfungsbehörde vorgelegt und auch nicht veröffentlicht. Zusätzlich erkläre ich, dass für die Rechtschreibprüfung KI-Tools verwendet wurden.

Osnabrück, _____ Unterschrift: _____

Urheberrechtliche Einwilligungserklärung

Hiermit erkläre ich, dass ich damit einverstanden bin, dass meine Arbeit zum Zwecke des Plagiatsschutzes bei der Fa. Ephorus BV bis zu 5 Jahren in einer Datenbank für die Hochschule Osnabrück archiviert werden kann. Diese Einwilligung kann jederzeit widerrufen werden.

Osnabrück, _____ Unterschrift: _____